Nonperturbative renormalization group preserving full-momentum dependence: Implementation and quantitative evaluation

F. Benitez
LPTMC, CNRS-UMR 7600, Université Pierre et Marie Curie, F-75252 Paris, France
Instituto de Fìsica, Facultad de Ciencias, Universidad de la República, 11400 Montevideo, Uruguay

J.-P. Blaizot
Institut de Physique Théorique, CEA-Saclay, F-91191 Gif-sur-Yvette, France

H. Chaté
Service de Physique de l'Etat Condensé, CEA-Saclay, F-91191 Gif-sur-Yvette, France

B. Delamotte
LPTMC, CNRS-UMR 7600, Université Pierre et Marie Curie, F-75252 Paris, France

R. Méndez-Galain and N. Wschebor
Instituto de Fìsica, Facultad de Ingeniería, Universidad de la República, 11000 Montevideo, Uruguay
(Received 12 October 2011; revised manuscript received 16 December 2011; published 28 February 2012)

We present the implementation of the Blaizot-Méndez-Wschebor approximation scheme of the nonperturbative renormalization group we present in detail, which allows for the computation of the full-momentum dependence of correlation functions. We discuss its significance and its relation with other schemes, in particular, the derivative expansion. Quantitative results are presented for the test ground of scalar $O(N)$ theories. Besides critical exponents, which are zero-momentum quantities, we compute the two-point function at criticality in the whole momentum range in three dimensions and, in the high-temperature phase, the universal structure factor. In all cases, we find very good agreement with the best existing results.

DOI: 10.1103/PhysRevE.85.026707 PACS number(s): 05.10.Cc, 11.10.Gh, 64.60.ae, 64.60.fd

I. INTRODUCTION

The exact or nonperturbative renormalization group (NPRG), as formulated in the seminal work of Wetterich [1], leads to an exact flow equation for an effective action (see also Refs. [2,3] for the original formulation of the NPRG). In general, this equation cannot be solved but offers the possibility for developing approximation schemes qualitatively different from those based on perturbation theory, allowing, in particular, to tackle nonperturbative problems.

The derivative expansion (DE) is such a scheme: Based on an expansion of the running effective action in terms of gradients of the fields, it has been applied successfully to a variety of physical problems, in condensed matter, particle physics, or statistical mechanics (see, e.g., Ref. [4]). The DE scheme allows us to calculate not only universal quantities, such as critical exponents [4,5], but also nonuniversal quantities defined at vanishing momenta, such as phase diagrams (see, e.g., Ref. [6]). However, it does not give access to the full-momentum dependence of correlation functions, something desirable in many situations.

The present paper deals with another nonperturbative scheme, namely, with the strategy proposed by Blaizot, Méndez-Galain, and Wschebor (BMW) in Refs. [7,8], which is reminiscent of earlier attempts by Parola and Reatto [9]. The BMW scheme, like all NPRG schemes, makes use of a regulating or cutoff function $R_k(q)$, which renders all vertex functions smooth and ensures that the RG flow at scale k involves the integration of fluctuations with momenta q *at most* on the order of k. At order s, the approximation consists of setting the internal momentum q to zero in the n-point functions $\Gamma_k^{(n)}$ with $n > s$ leaving a closed set of flow equations. In Ref. [7], it was shown that the BMW method encompasses any perturbative results, provided it is pushed to high-enough orders of s. For the particular $s = 2$ case studied in the following, it is one-loop exact for the two-point function. In Ref. [7], it has also been shown that, in the $N \to \infty$ limit of the $O(N)$ scalar models, the BMW scheme is no longer an approximation, thus allowing the computation of any correlation function.

The BMW approximation scheme has been applied to $O(N)$ models with success in simplified versions involving either the expansions in the fields [10] or an approximated propagator [11]. In this paper, we provide a full account of the practical implementation of the method without further simplifications. We also detail and extend the results recently obtained at order $s = 2$ [12]. In particular, we extract the universal scaling function governing the critical region. At the quantitative level, we find very good agreement with the best existing results.

The remainder of this paper is organized as follows: After a general presentation of the NPRG framework (Sec. II), we detail the BMW approximation scheme in Sec. III and show how to implement it in practice in Sec. IV. In Sec. V, we report on the results obtained at criticality (critical exponent values, shape of the two-point function, etc.), whereas, in Sec. VI, we compare the universal scaling function obtained in the whole critical region to existing results. In Sec. VII, we show how

the BMW results shed new light on the derivative expansion approximation scheme, and we discuss in particular its validity domain. Conclusions can be found in Sec. VIII, whereas the appendices gather technical material.

II. THE NPRG FRAMEWORK

For the sake of simplicity, in the following, we only discuss a scalar-field theory in the Ising universality class and defer the presentation of the equations that hold for general $O(N)$-symmetric models to Appendix D.

We, thus, consider the usual partition function,

$$\mathcal{Z}[j] = \int \mathcal{D}\varphi e^{-S+\int_x j\varphi}, \tag{1}$$

where S is the classical action, which, apart from being Z_2 invariant, is an *a priori* arbitrary function (possibly nonpolynomial). In the following, it is understood that, if necessary, the functional integral in Eq. (1) is regularized by a UV cutoff at a scale Λ (for instance, a lattice with spacing $a \sim \Lambda^{-1}$) so that S is associated with this scale. Notice that the usual ϕ^4 model whose action reads

$$S = \int d^dx \left\{ \frac{1}{2}(\partial_\mu\varphi)^2 + \frac{r}{2}\varphi^2 + \frac{u}{4!}\varphi^4 \right\} \tag{2}$$

belongs to this class but that, in the following, we do not restrict our paper to this particular case (as explained below, S is nothing but the initial condition of the RG flow at the UV scale Λ and, thus, can take any form). In Eq. (1), $j(x)$ is an external source, and $\int_x j\varphi$ is shorthand for $\int d^dx\, j(x)\varphi(x)$.

The NPRG strategy is to build a family of theories indexed by a momentum scale parameter k such that fluctuations are taken smoothly into account as k is lowered from the UV scale Λ down to 0 [1,2,4,13–17]). In practice, this is achieved by adding to the original Euclidean action S a k-dependent quadratic (masslike) term of the form

$$\Delta S_k[\varphi] = \frac{1}{2}\int_q R_k(q)\varphi(q)\varphi(-q), \tag{3}$$

with

$$\int_q \equiv \int \frac{d^dq}{(2\pi)^d},$$

so that the partition function at scale k reads

$$\mathcal{Z}_k[j] = \int \mathcal{D}\varphi e^{-S-\Delta S_k+\int_x j\varphi}. \tag{4}$$

The cutoff function $R_k(q)$ is chosen so that: (i) It is on the order of k^2 for $q \ll k$, which effectively suppresses the modes $\varphi(q \ll k)$; (ii) it vanishes for $q \gg k$, leaving the modes $\varphi(q)$ with $q \gg k$ unaffected. Thus, when $k = \Lambda$, $R_k(q)$ is on the order of Λ^2 for all $q \leqslant \Lambda$, and fluctuations essentially are frozen. On the other hand, when $k = 0$, $R_k(q)$ vanishes identically so that $\mathcal{Z}_{k=0} = \mathcal{Z}$, and the original theory is recovered. The specific form of the cutoff function $R_k(q)$ will be specified later.

Following Wetterich [1], an effective action at scale k, $\Gamma_k[\phi]$, is defined through the (slightly modified) Legendre transform,

$$\Gamma_k[\phi] + \ln\, \mathcal{Z}_k[j] = \int_x j\phi - \Delta S_k[\phi], \tag{5}$$

where $\phi(x) = \delta\, \ln\, \mathcal{Z}_k[j]/\delta j(x)$. This effective action obeys the exact flow equation [1] (up to a volume factor),

$$\partial_t\Gamma_k[\phi] = \frac{1}{2}\int_q \frac{\partial_t R_k(q)}{\Gamma_k^{(2)}[q,-q;\phi] + R_k(q)}, \tag{6}$$

where $t = \ln\, k/\Lambda$ and, thus, $\partial_t \equiv k\partial_k$ and $\Gamma_k^{(2)}[q,-q;\phi]$ is the Fourier transform of the second functional derivative of $\Gamma_k[\phi]$,

$$\Gamma_k^{(2)}[x_1,x_2;\phi] \equiv \frac{\delta^2\Gamma_k}{\delta\phi(x_1)\delta\phi(x_2)}. \tag{7}$$

Thus, $\{\Gamma_k^{(2)}[q,-q;\phi] + R_k(q)\}^{-1}$ is the full propagator in the presence of the field $\phi(x)$. The initial condition of the flow equation (6) is specified at the microscopic scale $k = \Lambda$ where fluctuations are frozen by ΔS_k so that $\Gamma_{k=\Lambda}[\phi] \approx S[\phi]$. The effective action $\Gamma[\phi]$ of the original scalar-field theory defined by Eq. (1) is obtained as the solution of Eq. (6) for $k \to 0$ (that is, $t \to -\infty$), at which point, $R_k(q)$ vanishes identically.

When ϕ is constant, the functional $\Gamma_k[\phi]$ reduces, to within a volume factor Ω, to a simple function of ϕ called the effective potential $V_k(\phi)$,

$$\Gamma_k[\phi] = \Omega V_k(\phi), \quad \phi \text{ const.} \tag{8}$$

The flow equation for V_k reads

$$\partial_t V_k(\rho) = \frac{1}{2}\int_q \partial_t R_k(q) G_k(q;\phi), \tag{9}$$

where

$$G_k^{-1}(q;\phi) = \Gamma_k^{(2)}(q;\phi) + R_k(q) \tag{10}$$

(see Appendix A for notation).

Let us now consider the flow of n-point functions. By taking two functional derivatives of Eq. (6), letting ϕ be constant, and Fourier transforming, one obtains the equation for the two-point function,

$$\begin{aligned}\partial_t\Gamma_k^{(2)}(p;\phi) = \int_q \partial_t R_k(q) G_k^2(q;\phi) \Big\{ & \Gamma_k^{(3)}(p,q,-p-q;\phi) \\ & \times G_k(q+p;\phi)\Gamma_k^{(3)}(-p,p+q,-q;\phi) \\ & -\frac{1}{2}\Gamma_k^{(4)}(p,-p,q,-q;\phi)\Big\}.\end{aligned} \tag{11}$$

The flow equations (9) and (11) are the first equations of an infinite tower of coupled equations for the n-point functions: Typically, the equation for $\Gamma_k^{(n)}$ involves all the vertex functions up to $\Gamma_k^{(n+2)}$. Thus, approximations and truncations are needed to obtain any practical result.

The presence of a sufficiently smooth cutoff function $R_k(q)$, (i) ensures that the $\Gamma_k^{(n)}$'s remain regular functions of the momenta and (ii) limits, through the term $\partial_t R_k(q)$, the internal momentum q in equations, such as Eq. (11), to $q \lesssim k$. These key remarks allow for approximations without equivalence in more traditional frameworks and, thus, constitute one of the specificities of the NPRG approach.

The approximation scheme most widely used is the derivative expansion, which is entirely based on the above remarks about the analyticity of the vertex functions. It amounts to formulating an ansatz for $\Gamma_k[\phi]$ as an expansion in the derivatives of the field. For instance, at order ∇^2,

$$\Gamma_k[\phi] = \int_x \left[V_k(\phi) + \frac{1}{2} Z_k(\phi) (\nabla\phi)^2 + O(\nabla^4) \right]. \quad (12)$$

The flow equation (6) then reduces to a set of two coupled partial differential equations for the functions $V_k(\phi)$ and $Z_k(\phi)$. During the years. the derivative expansion scheme has produced a wealth of remarkable results (see, e.g., Refs. [4,6,18]), but it does not allow accessing the full-momentum dependence of the vertex functions, something inherently possible within the BMW scheme. We discuss this point in Sec. VII, where we show how the BMW approach sheds new light on the derivative expansion.

III. THE BMW APPROXIMATION SCHEME

The BMW scheme at order s aims at preserving the full-momentum dependence of $\Gamma_k^{(s)}$ and approximating the momentum dependence of $\Gamma_k^{(s+1)}$ and $\Gamma_k^{(s+2)}$ in the flow equation of $\Gamma_k^{(s)}$ [7,8].

For uniform fields, the following formula:

$$\Gamma_k^{(s+1)}(\{p_i\}, p_{s+1} = 0; \phi) = \partial_\phi \Gamma_k^{(s)}(\{p_i\}; \phi), \quad (13)$$

where index i runs between 1 and s, allows reducing the order of the vertex functions as soon as one momentum vanishes.

The BMW approximation relies on this formula, together with the analyticity of the vertex functions and the fact that the internal momentum q in the flow equations, such as Eq. (11) effectively is limited to $q \lesssim k$. The BMW scheme at order s, thus, consists of:

(i) neglecting the dependence on the internal momentum q of $\Gamma_k^{(s+1)}$ and $\Gamma_k^{(s+2)}$:

$$\Gamma_k^{(s+1)}(p_1, \ldots, p_s - q, q; \phi) \to \Gamma_k^{(s+1)}(p_1, \ldots, p_s, 0; \phi), \quad (14)$$

and similarly for $\Gamma_k^{(s+2)}(p_1, \ldots, p_s, -q, q; \phi)$;

(ii) using Eq. (13), which allows us to express the approximated expressions (14) as derivatives of $\Gamma_k^{(s)}$ with respect to ϕ, thereby closing the hierarchy of RG equations at the level of the flow equation for $\Gamma_k^{(s)}$.

Note that the substitution in Eq. (14) is *not* applied to the q dependence already present in the initial (also called bare) n-point functions [7,8]. Thus, for instance, at the lowest level of the approximation ($s = 0$, the local potential approximation discussed below in Sec. III A), one leaves the initial q^2 dependence of $\Gamma_k^{(2)}(q)$ untouched. This ensures, in particular, that the propagator is one-loop exact.

The accuracy of the scheme depends on the rank s at which one operates the approximation. Obviously, the implementation becomes increasingly complicated as s grows. Later, we will show that good results can be obtained with low order truncations, i.e., at the levels $s = 0$ and $s = 2$. The corresponding approximations are discussed in the next subsections.

A. $s = 0$: The local potential approximation

The local potential approximation (LPA) often is seen as the leading order of the DE approximation scheme [4,17]. In this subsection, we show that it also can be seen as the zeroth order of the BMW scheme.

The BMW approximation for $s = 0$, consists of neglecting the (nontrivial) q dependence of the two-point function in the flow equation (9) of the zero-point function, that is, of the effective potential V_k. That is, one substitutes

$$\Gamma_k^{(2)}(q; \phi) \to q^2 + \Gamma_k^{(2)}(0; \phi) = q^2 + \partial_\phi^2 V_k. \quad (15)$$

Note that the equality in the equation above is a particular case of the general relation (13). By substituting Eq. (15) in Eq. (9), one gets the equation for the potential in the form

$$\partial_t V_k(\rho) = \frac{1}{2} \int_q \frac{\partial_t R_k(q)}{q^2 + R_k(q) + \partial_\phi^2 V_k}. \quad (16)$$

This is the flow equation for the potential obtained within the DE truncated at the LPA level. There, Eq. (9) is derived by computing the propagator from the ansatz,

$$\Gamma_k^{\mathrm{LPA}}[\phi] = \int d^d x \left\{ \frac{1}{2} (\nabla\phi)^2 + V_k(\phi) \right\}, \quad (17)$$

by inserting it in Eq. (9).

Since it allows for the calculation of the entire effective potential, the LPA provides information on *all* the $\Gamma_k^{(n)}$'s at once but only for vanishing external momenta: These functions are indeed those that are obtained by taking the derivatives of the effective potential, i.e.,

$$\Gamma_k^{(n)}(0, \ldots, 0; \phi) = \partial_\phi^n V_k. \quad (18)$$

Non-trivial -momentum dependence will appear at the next level of approximation to be described in the next subsection.

B. First order with full-momentum dependence: $s = 2$

The order of $s = 2$ is the first order of the BMW approximation where a non-trivial-momentum dependence is kept. The loop momentum q in the three- and four-point functions on the right hand side of Eq. (11) is neglected, and Eq. (13) is applied. The flow equation for $\Gamma_k^{(2)}(p; \phi)$ then becomes a closed equation,

$$\partial_t \Gamma_k^{(2)} = J_3(p; \phi) \left(\partial_\phi \Gamma_k^{(2)} \right)^2 - \tfrac{1}{2} I_2(\phi) \partial_\phi^2 \Gamma_k^{(2)}, \quad (19)$$

where we have introduced the notation,

$$\begin{aligned} I_n(\phi) &\equiv J_n(p = 0; \phi), \\ J_n(p; \phi) &\equiv \int_q \partial_t R_k(q) G_k(p + q; \phi) [G_k(q; \phi)]^{n-1}. \end{aligned} \quad (20)$$

Again, as is the case for the LPA, the approximation at $s = 2$ provides information on *all* the n-point functions. This time, the n-point functions depend on a single momentum. They may be obtained as derivatives of the two-point function, according to

$$\Gamma_k^{(n)}(p, -p, 0, \ldots, 0; \phi) = \partial_\phi^{n-2} \Gamma_k^{(2)}(p; \phi), \quad (21)$$

which may be viewed as a generalization of Eq. (18). Thus, for instance, the momentum dependence that remains within

the three- and four-point vertices in Eq. (19) is indeed that of the two-point function itself.

At this point, an important subtlety appears, coming from the fact that the flow of the potential (or of its second derivative) can be calculated either from Eq. (9) in which $G_k(q;\phi)$ is obtained from Eqs. (19) and (10), or from Eq. (19) directly at $p=0$, since $\Gamma_k^{(2)}(0;\phi)=\partial_\phi^2 V_k$. If no approximations were made, both results would be identical. However, once approximations are performed, as is the case here, both results do not coincide.

At any order of s of the BMW approximation scheme, the same ambiguity takes place for any correlation function $\Gamma_k^{(n)}$ up to $n=s-1$. Given the fact that the approximation is imposed only on the flow equation of $\Gamma_k^{(s)}$ and not on those of $\Gamma_k^{(n)}$ with $n<s$, it is natural to compute these functions from their own flow equation (which is exact) and not from the flow equation of $\Gamma_k^{(s)}$ (which is approximate).

One then subtracts the parts of it that can be expressed in terms of lower order correlation functions from $\Gamma_k^{(s)}$ and performs the BMW approximation in the equation for the *difference*. For $s=2$, this amounts to compute the potential from Eq. (9) and to implement the BMW approximation on $\Gamma_k^{(2)}(p;\phi)-\Gamma_k^{(2)}(0;\phi)$.

The rationale behind this choice is that computing the flow of $\partial_\phi^2 V_k$ from the equation for $\Gamma_k^{(2)}(p;\phi)$ at $p=0$ would imply two approximations: Eq. (19) for $\Gamma_k^{(2)}(p;\phi)$ is itself approximated, and propagators and vertices on its right hand side also are approximated. On the contrary, Eq. (9) for the potential is formally exact and only the propagator used in it is approximated. This general consideration can be made more concrete in the perturbative regime: The function $\Gamma_k^{(2)}(p;\phi)$ obtained from Eq. (19) is one-loop exact and so is $\Gamma_k^{(2)}(p=0;\phi)=\partial_\phi^2 V_k$. When the corresponding propagator, computed from Eq. (10), is inserted in Eq. (9), the obtained potential becomes two-loop exact. By generalizing the above subtraction procedure at higher orders, similar perturbative considerations can be performed: At order $s=2s'$ of the BMW scheme, the potential computed from Eqs. (9) and (10) is $(s'+1)$-loop exact, $\Gamma_k^{(2)}$ computed from Eq. (11) is s'-loop exact, and so on. We, thus, expect that implementing the BMW approximation only on the part of $\Gamma_k^{(s)}$, which is genuinely at order s, will have a decreasing impact on the lower order correlation functions as s grows.

In practice, for $s=2$, we rewrite

$$\Gamma_k^{(2)}(p;\phi)=p^2+\Delta_k(p;\phi)+\partial_\phi^2 V_k(\phi), \tag{22}$$

where $V_k(\phi)$ is obtained by solving Eq. (9), and moreover, for numerical convenience (see below), the initial p^2 term has been extracted. The BMW approximation is implemented only on the flow for Δ_k. The equation for $\Delta_k(p;\phi)$ can be deduced from Eq. (19) by subtracting its $p=0$ form

$$\begin{aligned}\partial_t\Delta_k(p,\rho)=&\,2\rho J_3(p,\rho)[u_k(\rho)+\Delta_k'(p,\rho)]^2-2\rho I_3(\rho)u_k^2(\rho)\\&-\tfrac{1}{2}I_2(\rho)[\Delta_k'(p,\rho)+2\rho\Delta_k''(p,\rho)],\end{aligned} \tag{23}$$

with

$$\rho=\tfrac{1}{2}\phi^2, \tag{24}$$

$$m_k^2(\rho)\equiv\Gamma_k^{(2)}(0,\rho)=\partial_\phi^2 V_k, \tag{25}$$

$$u_k(\rho)\equiv\partial_\rho m_k^2(\rho), \tag{26}$$

and the symbol $'$ denotes the derivative with respect to ρ.

In closing this section, let us mention that the relationships between the BMW scheme at order $s=2$ and, on one hand, the large N expansion and, on the other hand, the DE, are discussed respectively in Secs. V C and VII.

IV. IMPLEMENTATION AT CRITICALITY

In order to efficiently treat the low-momentum region at criticality and, in particular, to accurately capture the fixed-point structure, we first introduce dimensionless and renormalized variables to be denoted with a tilde. We, thus, introduce a renormalization factor Z_k, which reflects the finite change in normalization of the field between UV scale Λ and scale k. Within the DE at $O(\nabla^2)$, this factor describes the overall variation with k of the *function* $Z_k(\phi)$ in Eq. (12). Here, we define the factor Z_k by

$$Z_k=\left.\frac{\partial\Gamma_k^{(2)}(p,\rho)}{\partial p^2}\right|_{p=p_0,\,\rho=\rho_0}, \tag{27}$$

where p_0 and ρ_0 are *a priori* arbitrary. Notice that we assume in the following that the scaling dimension of ϕ is $d/2-1$ in mass units as usual, so that Z_k is dimensionless. From Z_k, we define the running anomalous dimension η_k by

$$\eta_k=-k\partial_k\,\ln\,Z_k. \tag{28}$$

As usual, it is convenient to measure all quantities in units of the running scale k. Thus, momenta are rescaled naturally according to $p=k\tilde{p}$, and other quantities are made dimensionless by dividing them by appropriate powers of k (and possibly conveniently extracting numerical factors). Thus, we define

$$\begin{aligned}\rho=K_d k^{d-2}Z_k^{-1}\tilde{\rho},\quad m_k^2(\rho)=Z_k k^2\tilde{m}_k^2(\tilde{\rho}),\\ u_k(\rho)=Z_k^2 k^{4-d}K_d^{-1}\tilde{u}_k(\tilde{\rho}),\end{aligned} \tag{29}$$

where K_d is a constant originating from angular integrals,

$$K_d^{-1}=2^{d-1}d\pi^{d/2}\Gamma(d/2). \tag{30}$$

We also set

$$G_k(p,\rho)=\frac{1}{Z_k k^2}\tilde{G}_k(\tilde{p},\tilde{\rho}), \tag{31}$$

$$J_n(p,\rho)=K_d\frac{k^{d+2-2n}}{Z_k^{n-1}}\tilde{J}_n(\tilde{p},\tilde{\rho}). \tag{32}$$

Instead of $R_k(q)$, it is convenient to work with a dimensionless cutoff function considered as a function of $y=q^2/k^2$,

$$r(y)\equiv\frac{R_k(q)}{q^2Z_k}. \tag{33}$$

Now, we note that, as $p\to 0$ at fixed k, $\Delta_k(p,\rho)\propto p^2$. This p^2 dependence may generate numerical instabilities in the equation for Δ (once transformed to dimensionless variables).

In order to avoid these, we found it convenient to introduce the renormalized and dimensionless two-point function $\tilde{Y}_k(\tilde{p},\tilde{\rho})$,

$$1+\frac{\Delta_k(p,\rho)}{p^2}\equiv Z_k[1+\tilde{Y}_k(\tilde{p},\tilde{\rho})], \tag{34}$$

The function $\tilde{Y}_k(\tilde{p},\tilde{\rho})$ is a slowly varying function of $\tilde{p}$, and its flow equation is regular. This equation is obtained easily from the flow equation for $\Delta(p,\rho)$, Eq. (23). It reads

$$\begin{aligned}\partial_t\tilde{Y}_k &= \eta_k(1+\tilde{Y}_k)+\tilde{p}\,\partial_{\tilde{p}}\tilde{Y}_k-(2-d-\eta_k)\tilde{\rho}\tilde{Y}_k'\\ &\quad+2\tilde{\rho}\tilde{p}^{-2}\big[(\tilde{p}^2\tilde{Y}_k'+\tilde{u}_k)^2\tilde{J}_3-\tilde{u}_k^2\tilde{I}_3\big]\\ &\quad-\tilde{I}_2(\tilde{Y}_k'/2+\tilde{\rho}\tilde{Y}_k'').\end{aligned} \tag{35}$$

The normalization condition (27) now is expressed as

$$\tilde{Y}_k(\tilde{p}=\tilde{p}_0,\ \tilde{\rho}=\tilde{\rho}_0)=0,\quad \forall\, k. \tag{36}$$

The equation for $\tilde{Y}_k(\tilde{p},\tilde{\rho})$ needs to be completed by the flow equation for the dimensionless effective potential $\tilde{V}_k(\tilde{\rho})=k^{-d}V_k(\rho)$, or rather, the equation for its derivative $\tilde{W}_k(\tilde{\rho})=\tilde{V}_k'(\tilde{\rho})$, which is more convenient since $\tilde{V}_k$ contains a trivial constant part that induces a numerical divergence. The equation for $\tilde{W}_k$ reads

$$\partial_t\tilde{W}_k(\tilde{\rho})=-(2-\eta_k)\tilde{W}_k(\tilde{\rho})+(d-2+\eta_k)\tilde{\rho}\tilde{W}_k'(\tilde{\rho})+\tfrac{1}{2}\tilde{I}_1'(\tilde{\rho}). \tag{37}$$

Finally, η_k in Eq. (35) is determined implicitly by inserting the renormalization condition (36) in the flow equation of $\tilde{Y}_k(\tilde{p},\tilde{\rho})$ and evaluating the right hand side at $\tilde{\rho}=\tilde{\rho}_0$ and $\tilde{p}=\tilde{p}_0$.

In principle, and if no approximations were performed, no physical quantity would depend on the choice of $\tilde{\rho}_0$ and $\tilde{p}_0$ nor on the relatively free choice of the cutoff function $r(y)$. In practice, the BMW scheme, as any approximation scheme, introduces spurious dependences on these choices. Below, we use the one-parameter family of cutoff functions,

$$r(y)=\frac{\alpha}{e^y-1}, \tag{38}$$

and study the dependence of our results on $\tilde{\rho}_0$, $\tilde{p}_0$, and α [19].

We numerically solved the flow equations having, as an initial condition at scale Λ, a ϕ^4-like classical action. More precisely, we took

$$\begin{aligned}\tilde{W}_\Lambda(\tilde{\rho}) &= r/\Lambda^2+(u/3)\Lambda^{d-4}K_d\tilde{\rho},\\ \tilde{Y}_\Lambda(\tilde{\rho},\tilde{p}) &= 0,\end{aligned} \tag{39}$$

searching, at fixed u, for the critical point by dichotomy on parameter r. We set $\tilde{u}\equiv u\Lambda^{d-4}K_d$.

The numerical resolution is performed on a fixed regular $(\tilde{p},\tilde{\rho})$ grid, with $0\leqslant\tilde{p}\leqslant\tilde{p}_{\max}$ and $0\leqslant\tilde{\rho}\leqslant\tilde{\rho}_{\max}$. With our choice of cutoff function, we have found that the contribution of the momentum interval $\tilde{q}\in[4,\infty]$ to the integrals $\tilde{I}_n$ and $\tilde{J}_3$ is extremely small, and we, thus, have neglected it by restricting the integration domain to $\tilde{q}\in[0,4]$. When computing the double integrals $\tilde{J}_3(\tilde{p},\tilde{\rho})$, we need to evaluate $\tilde{Y}$ for momenta $\tilde{p}+\tilde{q}$ beyond $\tilde{p}_{\max}$. In such cases, we set $\tilde{Y}(\tilde{p}>\tilde{p}_{\max})=\tilde{Y}(\tilde{p}_{\max})$, an approximation checked to be excellent for $\tilde{p}_{\max}\geqslant 5$. To access the full-momentum dependence, we also calculate $\Gamma_k^{(2)}(p,\tilde{\rho})$ at a set of fixed freely chosen external p values. For a given such p, p/k is within the grid at the beginning of the flow. This is no longer so when $k<p/\tilde{p}_{\max}$; then, we switch to the dimensionful version of Eq. (35) and set $J_3(p,\tilde{\rho})=G(p,\tilde{\rho})J_2(0,\tilde{\rho})$, an excellent approximation when $p>k\,\tilde{p}_{\max}$.

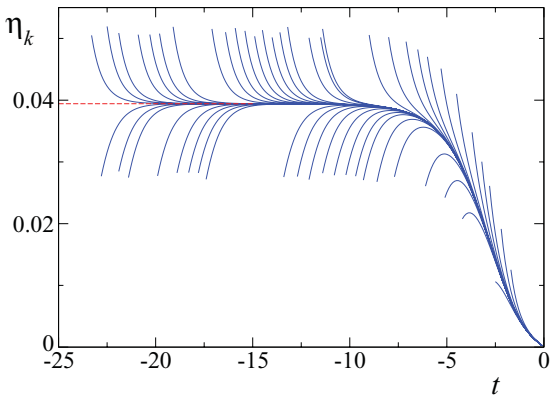

FIG. 1. (Color online) Example of the dichotomy procedure used for reaching the fixed point ($N=1$, $d=3$, $\tilde{u}=6\times10^{-2}$, $\tilde{\rho}_0=0$, $\tilde{p}_0=0$, and $\alpha=2.25$). The plot shows the running anomalous dimension η_k as a function of $t=\ln(k/\Lambda)$. Each curve corresponds to a different initial value of r [see Eq. (39)]. The red dashed line indicates the estimated asymptotic value $\eta\simeq0.039\,43$.

We found that the simplest time stepping (that is, explicit Euler), a finite-difference evaluation of derivatives on a regular $(\tilde{p},\tilde{\rho})$ grid, and the use of Simpson's rule to calculate integrals are sufficient to produce stable and fast-converging results. For all the quantities calculated, the convergence to, at least, three significant digits is reached with a $(\tilde{p},\tilde{\rho})$ grid of 50×60 points and elementary steps $\delta\tilde{p}=0.1$ and $\delta\tilde{\rho}=0.1$. With such a grid, a typical run takes a few minutes on a current personal computer. The step in $t=\ln k/\Lambda$ is $\Delta t=10^{-4}$, and the flow is run down to $t\sim-20$. In order to find the fixed point, we performed a simple dichotomy procedure on the bare (initial) mass $m_\Lambda^2=r/\Lambda^2$ at fixed u, by studying the flow of $\tilde{W}_k(0)$. Figure 1 illustrates the flow of η_k as one approaches the fixed point.

V. RESULTS AT CRITICALITY

Although the main goal of the BMW method is to provide access to full-momentum dependence, it can, of course, also be used to compute critical exponents and other zero-momentum quantities [12]. In this section, where we turn to the $O(N)$ models (with general N), we provide details on the calculation of the critical exponents and check their robustness with respect to variations in the different parameters of the method, such as the numerical resolution, the choice of the cutoff function, and the location of the normalization point $(\tilde{\rho}_0,\tilde{p}_0)$.

Since we focus here on the regime of small momenta, it is convenient to take, as an initial condition [see Eq. (39)], a value of the dimensionless coupling $\tilde{u}$ not too small compared to 1 in order to initialize the flow far from the Gaussian fixed point $\tilde{u}=0$ and, thus, to quickly approach the infrared (IR) fixed point. This is useful not only because of the shortened time needed to reach the critical regime, but also because otherwise, due to the 16-digit precision used, our dichotomy procedure

does not allow for an accurate determination of the fixed point directly from initial parameters. The results to be presented below have been calculated for $\tilde{u} = 6 \times 10^{-2}/N$.

A. Numerical extraction of critical exponents

The anomalous dimension η comes out of the solution of the flow equations, which provide a direct estimate of η_k (Fig. 1). It can also be extracted from $\Gamma^{(2)}_{k=0}(p,\rho=0) \propto p^{2-\eta}$ at small momentum with the same result, although this is a much less practical way.

In the vicinity of the fixed point, the behavior of any dimensionless and renormalized quantity, such as the dimensionless mass $\tilde{m}_k^2 = \tilde{m}_k^2(\tilde{\rho}=0)$, is as follows (recall that $t = \ln k/\Lambda < 0$):

$$\tilde{m}_k^2 = \tilde{m}_*^2 + \tilde{m}_1^2 e^{-\frac{t}{\nu}} + \tilde{m}_2 e^{\omega t} + \tilde{m}_3 e^{\omega_2 t} + \cdots, \qquad (40)$$

with the universal critical exponent ν describing the departure from the critical surface and the correction to scaling exponents $\omega, \omega_2, \ldots$ describing the approach to the fixed point.

In practice, we use the flow (40) of the mass (the flow of η_k could also be used) to extract ν and ω [20]. We explore successive regions of t values where one of the exponentials in the equation above dominates. For instance, for t negative enough, we write

$$\ln|\partial_t \tilde{m}^2| \sim -\frac{t}{\nu} + \text{const} \qquad (41)$$

to find ν. To extract ω, we choose $|t|$ large enough but not so large as to leave the vicinity of the fixed point. We then write

$$\ln|\partial_t \tilde{m}^2| \sim \omega t + \text{const}. \qquad (42)$$

Notice that, away from the fixed point, the exponents thus determined, themselves depend weakly on t since, strictly speaking, Eq. (40) holds only in the infinitesimal vicinity of the fixed point. We, thus, obtain only (slowly) running exponents ν_k and ω_k. In practice, these exponents are calculated by taking the t derivative of Eqs. (41) and (42). Then, the procedure is repeated for a set of initial conditions that bring the system closer and closer to the critical point (we vary r at fixed u, see Fig. 2). The estimates of ν_k and ω_k saturate at their fixed-point values reflected in the plateau seen in Fig. 2 for ω_k (ω is more difficult to determine numerically than ν). Given such curves, one can extract even more accurate estimates from the (exponential) approach to the asymptotic plateau values, see the inset of Fig. 2.

With this method, we could, in principle, extract exponents with almost arbitrary numerical accuracy. In practice, however, only a few digits are significant: Our results suffer indeed from an uncertainty related to the choice of the cutoff function (see the next subsection); besides, it is not necessary to present results with an accuracy that far exceeds the deviation from those with which they are compared.

B. Dependence on renormalization point and regulator

Although, as explained above, the values of the critical exponents should, in principle, depend neither on the normalization point $(\tilde{p}_0, \tilde{\rho}_0)$ nor on the shape of the cutoff function $R_k(q)$, this is no longer the case once approximations are performed.

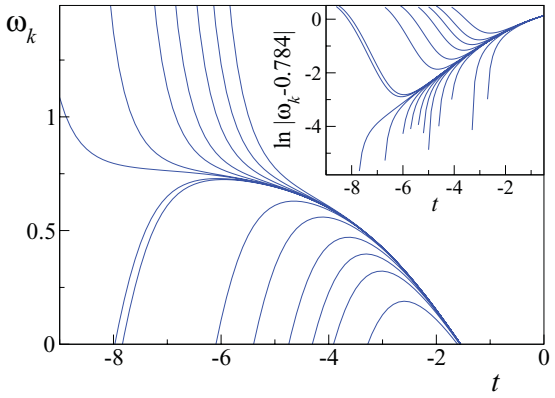

FIG. 2. (Color online) Running exponent ω_k ($d = 3$, $N = 1$, $\alpha = 2.25$, $p_0 = 0$, and $\rho_0 = 0$). Each curve corresponds to a different initial value of r [see Eq. (39)]. Inset, the exponential approach to the asymptotic exponent is used to estimate $\omega \simeq 0.784$.

In practice, we apply the principle of minimal sensitivity, searching for a local extremum of the physical quantities under study [19,21] in a reasonable subspace of values taken by α [the parameter of the cutoff function (38)], $\tilde{p}_0$, and $\tilde{\rho}_0$. Then, it is expected that the corresponding values are optimal in the sense that they show, locally, the weakest dependence on the above parameters.

Here, we first notice that, at fixed α and $\tilde{\rho}_0$, the dependence of our estimates on $\tilde{p}_0$ is much weaker than that found by varying α and $\tilde{\rho}_0$. Figure 3 shows the variation in the anomalous dimension η with α for two typical values of N in three dimensions. As in all other cases studied, we observe the existence of a unique extremum for a value of α that we call α^* in the following. Below, we always use these extremum values to report our best estimates for the critical exponents. Note that we do not show the variations in the exponents with $\tilde{\rho}_0$ as they can be shown to be equivalent to those with α [22].

C. Results for the critical exponents

We now present our results for the critical exponents of the scalar $O(N)$ models in $d = 3$. They have been obtained with a two-dimensional grid in $\tilde{\rho}$ and $\tilde{q}$ with $n_\rho = 51$ points in the $\tilde{\rho}$

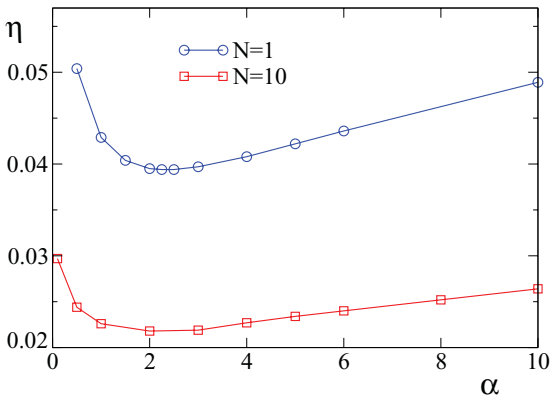

FIG. 3. (Color online) η as a function of the cutoff parameter α for $N = 1$ and $N = 10$ ($d = 3$, $\tilde{\rho}_0 = 0$, and $\tilde{p}_0 = 0$).

TABLE I. Results for the anomalous dimension η in $d = 3$, compared with results obtained within the DE at order $O(\nabla^2)$, field theory (FT), and Monte Carlo (MC) methods.

N	BMW	DE	FT	MC
0	0.034	0.039 [28]	0.0272(3) [29]	0.0303(3) [30]
1	0.039	0.0443 [19]	0.0318(3) [29]	0.03627(10) [31]
2	0.041	0.049 [28]	0.0334(2) [29]	0.0381(2) [32]
3	0.040	0.049 [28]	0.0333(3) [29]	0.0375(5) [33]
4	0.038	0.047 [28]	0.0350(45) [34]	0.0365(10) [35]
10	0.022	0.028 [28]	0.024 [36]	
100	0.0023	0.0030 [28]	0.0027 [26]	
$O(1/N)$	$0.23/N$		$0.270/N$ [26]	

direction, $n_q = 60$ points in $\tilde{q}$, and with $\tilde{q}_{\max} = 4$, $\tilde{p}_{\max} = 6$, and $\tilde{\rho}_{\max} = 5N$. Tables I–III contain our results for the critical exponents η, ν, and ω, together with some of the best estimates available in the literature, obtained either from MC or from resummed perturbative calculations [that we refer to as FT]. Our numbers all are given for the optimal values α^* of the cutoff parameter, and the digits quoted remain stable when α varies in the range $[\alpha^* - 1/2, \alpha^* + 1/2]$. The quality of these numbers is obvious: Our results for ν agree with previous estimates to within less than a percent, for all N; as for the values of η and ω, they are typically at the same distance from the MC and high-temperature series estimates (for instance, for $N = 1$ and $\nu = 0.6298(3)$ [23]) as the results from resummed perturbative calculations. Our numbers also compare favorably with those obtained at order ∇^2 in the DE scheme [19].

In the limit of large N, the BMW scheme becomes exact for the two-point function for $s \geqslant 2$ [7,8]. This generalizes the fact, shown in Ref. [24], that the LPA ($s = 0$) is exact in the large N limit for the effective potential. From Tables I–IV, it can be verified that the large N limit values $\eta = 0$, $\nu = 1$, and $\omega = 1$ are approached for large values of N.

We also can perform a $1/N$ expansion [25,26]. This already was performed in Ref. [11] where the BMW scheme was approximated further by the use of LPA propagators. As the LPA becomes exact in the large N limit, these results are unchanged at first order in $1/N$, except for the use of another type of regulator profile. An analytical study of the BMW equations in this limit provides the following values for the critical exponents at order $1/N$: $\eta = 0.23/N$ and $\nu = 1 - 1.034/N$, to be compared with the exact results [26] $\eta = 0.27/N$ and $\nu = 1 - 1.081/N$. In Ref. [11], the use of another regulator profile allowed us to obtain somewhat better results for η in this limit: $\eta = 0.25/N$. Notice that all these analytical results are recovered in our numerical solution for large values of N (notice, in fact, that terms at order $1/N^2$ already are very small for $N > 4$).

The two-dimensional case, for which exact results exist, provides a very stringent test of the BMW scheme. We focus here on the Ising model $N = 1$, which exhibits a standard critical behavior in $d = 2$ and the corresponding critical exponents. Notice that the perturbative method that works well in $d = 3$ fails here: For instance, the fixed-dimension expansion that provides the best results in $d = 3$ yields, in $d = 2$ and at five loops, $\eta = 0.145(14)$ [27] in contradiction with the exact value $\eta = 1/4$.[1] Instead, we find $\eta = 0.254$ and $\nu = 1.00$ in excellent agreement with the exact values $\eta = 1/4$ and $\nu = 1$. A more detailed study of $O(N)$ models in $d = 2$, at and out of criticality, will be presented in a separate paper.

D. The function $\Gamma^{(2)}$ at criticality and further tests at intermediate and large momenta

We now study the momentum dependence of the two-point function at criticality. In dimension three, the bare (initial) coupling constant u has the dimension of a momentum and, thus, sets a scale (the Ginzburg length $\xi_G \sim u^{1/(d-4)}$). Typically, there are three momentum domains for $\Gamma^{(2)}(p, \rho = 0)$ [11,12]:

(i) The IR domain defined by $p \ll u$ where $\Gamma^{(2)}(p) \sim u^\eta p^{2-\eta}$. In Fig. 4, we show that this behavior is well reproduced by our solution of the flow equation. To clearly see this regime on a large range of momenta, we have integrated the flow with an initial value of u not too far from the value of Λ, $\tilde{u} = 6.10^{-2}/N$.

(ii) The UV domain defined by $p \gg u$ (and $\Lambda \gg p$) where $\Gamma^{(2)}(p)$ can be studied perturbatively and is found to behave at two loops as $\Gamma^{(2)}(p) - p^2 \sim -(\mathcal{C}_N/96\pi^2)u^2 \ln p/u$ [with $\mathcal{C}_N = (N+2)/3$]. In Ref. [11], it was shown that, in the BMW approximation, and at large momenta, $\Delta(p, \rho = 0)$ behaves as $u^2 \ln(p/u)$, more precisely,

$$\frac{\partial \Delta_{k=0}(p,0)}{\partial |p|} = \mathcal{C}_N \frac{u^2}{2|p|} \int_{l,q} \partial_t R_k(l) G_0^2(l) G_0^2(q). \qquad (43)$$

The $u^2 \ln p/u$ behavior, thus, is retrieved, see Fig. 5, with a prefactor that, however, depends on $R_k(q)$. With the exponential cutoff function, Eq. (38), the prefactor can only be calculated numerically. We have studied its dependence on α

[1] It has been conjectured (see Ref. [55] and references therein), and this is confirmed by $1/N$ calculations, that the presence of nonanalytic terms in the flow of the ϕ^4 coupling u could be responsible for the discrepancy between exact and perturbative results in $d = 2$. According to Sokal, no problem should arise when all couplings, including the irrelevant ones, are retained in the RG flow, as performed here. This probably explains the quality of our results in $d = 2$.

TABLE II. Results for the critical exponent ν in $d = 3$, compared with results obtained within the DE at order $O(\nabla^2)$, FT, and MC methods.

N	BMW	DE	FT	MC
0	0.589	0.590 [28]	0.5886(3) [29]	0.5872(5) [37]
1	0.632	0.6307 [19]	0.6306(5) [29]	0.630 02(10) [31]
2	0.674	0.666 [28]	0.6700(6) [29]	0.6717(1) [32]
3	0.715	0.704 [28]	0.7060(7) [29]	0.7112(5) [33]
4	0.754	0.739 [28]	0.741(6) [34]	0.749(2) [35]
10	0.889	0.881 [28]	0.859 [36]	
100	0.990	0.990 [28]	0.989 [26]	
$O(1/N)$	$1 - 1.034/N$		$1-1.081/N$ [26]	

and have shown that there is an extremum around $\alpha \sim 5$ where the difference with the exact result is about 8%. Of course, this UV behavior shows up only if the bare coupling u is sufficiently small compared to Λ. We have chosen $\tilde{u} = 10^{-6}/N$ to have a large UV domain where this behavior is seen clearly. Note that, at small p, $\Gamma^{(2)}(p) - p^2 \sim p^{2-\eta}$, which is visible in Fig. 5, although this regime is approached very slowly.

(iii) The crossover between the IR and the UV domains. This regime of momentum is visible in both Figs. 4 and 5 for $p \simeq u$.

For purposes of probing the intermediate-momentum region between the IR and the UV, we have calculated the quantity,

$$c = -\frac{256}{uN}\zeta[3/2]^{-4/3}\int d^3p\left[\frac{1}{\Gamma^{(2)}(p)} - \frac{1}{p^2}\right], \qquad (44)$$

which is very sensitive to the crossover regime: The integrand in Eq. (44) is peaked at $p \sim (Nu)/10$ [38]. For this reason, the calculation of c has been used as a benchmark for nonperturbative approximations in the $O(N)$ model.

In the $O(2)$ case and for $d = 3$, this quantity determines the shift in the critical temperature of the weakly repulsive Bose gas [39] (notice that c is not defined for $d = 2$). Thus, it has been much studied recently using various methods even for other values of N. In particular, the large N limit for this quantity has been calculated analytically and has been found to be $c = 2.3$ [40]. In this paper, we have found the values for c for some representative values of N. Our results, compared to the best ones available in the literature (with their corresponding errors when available), are presented in Table IV. For all values of N where lattice and/or seven-loop resummed calculations exist, our results are within the error bars of those calculations (and comparable to those obtained from an approximation specifically designed for this quantity [8,41]), except for $N = 2$, where very precise lattice results are available. In the large N limit, one can see that our result differs from the exact value by less than 3%. Notice that the large N behavior of the quantity c is, in fact, at order $1/N$ [40], which, as we have seen, is not calculated exactly at this level of the BMW approximation.

Altogether, we can see that the BMW method at order $s = 2$ is able to reproduce the correct behavior of the two-point function at criticality in all momentum regimes. Note, in particular, that this is not the case of conformal field theoretical methods that only are able to capture the conformally invariant $p^{2-\eta}$ behavior at criticality but that can reproduce neither the UV behavior, corresponding to $u \ll p \ll \Lambda$, nor the crossover between the IR and the UV regions, corresponding to $p \simeq u$.

TABLE III. Results for the correction to scaling exponent ω in $d = 3$ compared with results obtained within the BMW method, FT, and MC results.

N	BMW	FT	MC
0	0.83	0.794(6) [29]	0.88 [30]
1	0.78	0.788(3) [29]	0.832(6) [31]
2	0.75	0.780(10) [29]	0.785(20) [32]
3	0.73	0.780(20) [29]	0.773 [33]
4	0.72	0.774(20) [34]	0.765 [35]
10	0.80		
100	1.00		

VI. SCALING FUNCTIONS

As an approximation of the NPRG, the BMW scheme allows us to investigate all momentum, temperature, and external magnetic-field regimes and is not restricted to the long distance physics at criticality. A particularly interesting

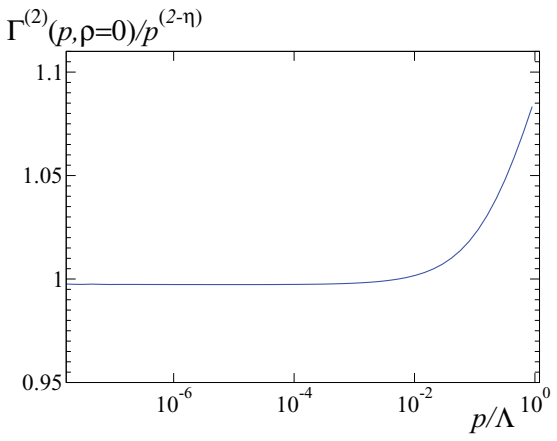

FIG. 4. (Color online) The ratio of the two-point function $\Gamma^{(2)}(p,0)$ and of $p^{2-\eta}$ at criticality as a function of p/Λ ($d = 3, N = 2$, $\alpha = 2$, $p_0 = 0$, and $\rho_0 = 0$). The normalization has been chosen so that this ratio starts close to 1 at small p. The bare (initial) dimensionless coupling is $\tilde{u} = 6.10^{-2}/N$.

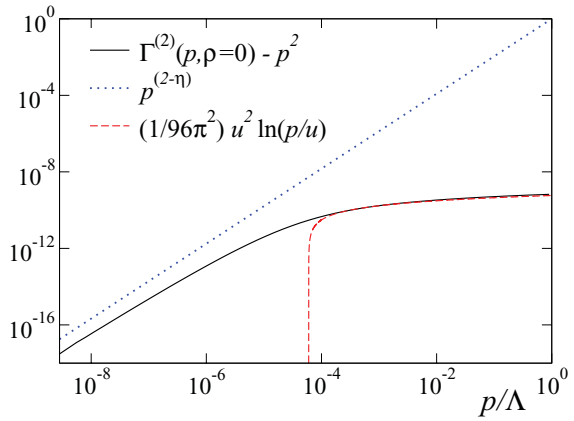

FIG. 5. (Color online) The difference $\Gamma^{(2)}(p,0) - p^2$ at criticality as a function of p/Λ, compared with its expected UV behavior $\sim u^2 \ln p/u$ ($d = 3$, $N = 2$, $\alpha = 2, p_0 = 0$, and $\rho_0 = 0$). The IR $p^{2-\eta}$ behavior is also shown (see text). The bare dimensionless coupling is $\tilde{u} = 10^{-6}/N$.

and *a priori* difficult regime is the critical domain where the correlation length is large but finite. In this case, an appropriately rescaled two-point function shows a universal behavior. As the BMW approximation allows for the calculation of genuine momentum-dependent quantities, the calculation of this scaling function and its comparison with the best available theoretical results from the literature and with experimental data represent one of the most stringent tests of the approximation.

In this paper, we consider the case $N = 1$ relevant, for instance, to describe the critical behavior of fluids near the liquid-gas critical point. Near this point and for $p \ll \xi_G^{-1} \sim u$, one expects the general scaling behavior,

$$G_{\pm}^{(2)}(p) = \chi g_{\pm}(p\xi), \tag{45}$$

with, by definition, $G^{(2)}$ as the density-density correlation function, $\chi^{-1} = \Gamma^{(2)}(p = 0)$ as the compressibility, and $\xi^{-2} = k^2 \tilde{m}_k^2$ with $k \to 0$ as the correlation length that diverges close to criticality with the ν critical exponent. Here, $\pm$ refers to the two phases, above and below the critical temperature, respectively. The functions $g_{\pm}(x)$, normalized so that

$$g^{-1}(x) = 1 + x^2 + O(x^4) \tag{46}$$

TABLE IV. Results for quantity c defined in the text.

N	BMW	Lattice	Seven loops [42]
1	1.15	1.09(9) [43]	1.07(10)
2	1.37	1.32(2) [44]	1.27(10)
		1.29(5) [45]	
3	1.50		1.43(11)
4	1.63	1.60(10) [43]	1.54(11)
10	2.02		
100	2.36		

are universal. Their limiting behavior is well known. For small x, they are well described by the Ornstein-Zernicke (mean-field) approximation,

$$g_{OZ}(x) = \frac{1}{1 + x^2}. \tag{47}$$

The corrections to the Ornstein-Zernicke behavior usually are parametrized as [46]

$$g_{\pm}(x)^{-1} = 1 + x^2 + \sum_{n=2} c_n^{\pm} x^{2n}. \tag{48}$$

The above behavior of $g_{\pm}(x)^{-1}$ is *a priori* valid only for $x < 1$, but since the coefficients c_n are very small, it turns out that the Ornstein-Zernicke approximation actually is valid over a wide range of x values as we see later. For large x (that is, $\xi \gg p^{-1}$), the scaling functions show critical behavior with an asymptotic anomalous power law decay,

$$g_{\pm}(x) \simeq \frac{C_1^{\pm}}{x^{2-\eta}}, \tag{49}$$

which allows for the experimental determination of the exponent η. This expression also allows for corrections as given by Fischer and Langer [47],

$$g_{\pm}(x) = \frac{C_1^{\pm}}{x^{2-\eta}} \left(1 + \frac{C_2^{\pm}}{x^{(1-\alpha)/\nu}} + \frac{C_3^{\pm}}{x^{1/\nu}} + \cdots \right). \tag{50}$$

Different approximate results for the universal scaling functions exist in the literature, obtained either by MC methods [46] or by the use of an analytical ansatz, interpolating between the two known limiting regimes (48) and (49), using ε expansion results (the Bray approximation [48]). Experimental results from neutron scattering in CO_2 near the critical point also exist [49].

In Bray's interpolation for the high-temperature phase, one assumes $g_+^{-1}(x)$ to be well defined in the complex x^2 plane with a branch cut in the negative real x^2 axis, starting at $x^2 = -r_+^2$ where $r_+^2 = 9M_{\rm gap}^2\xi^2 \equiv 9S_M$, following the theoretical expectation that the singularity of $g_+(x)$ nearest to the origin is the three-particle cut [48,49]. The parameter $M_{\rm gap}$ is the mass gap of the Minkowskian version of the model. For the ϕ^4 theory, it is known that the difference between mass gap and ξ^{-1} is very small and replacing one by the other corresponds to an error that is beyond the accuracy of our calculation [46]. Then, Bray's ansatz in the high-temperature phase (the only phase studied in the following) reads:

$$g_+^{-1}(x) = \frac{2 \sin \pi\eta/2}{\pi C_1^+} \times \int_{r_+}^{\infty} du\, F_+(u) \left[\frac{S_M}{u^2 - S_M} + \frac{x^2}{u^2 + x^2} \right], \tag{51}$$

where $F_+(u)$ is the spectral function, which satisfies $F_+(+\infty) = 1$ and $F_+(u) = 0$ for $u < r_+$ and $F_+(u) \geqslant 0$ for $u \geqslant r_+$. On top of this, one must impose $g^{-1}(0) = 1$, which fixes the value for C_1^+.

One must then specify $F_+(u)$. Bray [48] proposed the use of a spectral function with the exact Fischer-Langer asymptotic behavior of the type,

$$F_{+,B}(u) = \frac{P_+(u) - Q_+(u) \cot \frac{1}{2}\pi\eta}{P_+(u)^2 + Q_+(u)^2}, \tag{52}$$

where

$$P_+(u) = 1 + \frac{C_2^+}{u^\iota}\cos\frac{\pi\zeta}{2} + \frac{C_3^+}{u^{1/\nu}}\cos\frac{\pi}{2\nu},$$
$$Q_+(u) = \frac{C_2^+}{u^\iota}\sin\frac{\pi\zeta}{2} + \frac{C_3^+}{u^{1/\nu}}\sin\frac{\pi}{2\nu}, \tag{53}$$

with $\zeta \equiv (1-\alpha)/\nu$. This definition contains a certain number of parameters. On top of the critical exponents, which can be injected using either the BMW values or the best available results in the literature, one also must fix S_M^+, C_2^+, and C_3^+. For S_M^+, one can use the best estimate in the literature, given by the high-temperature expansion of improved models [51]. Bray proposed to fix $C_2^+ + C_3^+$ for its ε-expansion value $C_2^+ + C_3^+ = -0.9$ and, then, to determine C_1^+ by requiring $F_{+,B}(r_+) = 0$. These conditions allow for a little parameter tuning by adjusting the relative weight of the C_2^+ and C_3^+ parameters. When comparing our results with Bray's ansatz, we will use this freedom. We now turn to the scaling function computed by the BMW method.

In terms of the variables used in this paper, we find that

$$g^{-1}(p\xi) = \frac{(p\xi)^2 + \Delta(p\xi,0) + Z_k k^2 \tilde{m}_k^2(0)}{Z_k k^2 \tilde{m}_k^2(0)}, \tag{54}$$

when $k \to 0$. In this paper, for purposes of comparison with existing results, we only have computed the scaling function in the high-temperature phase. We have performed the calculation for different values of the correlation length (and, hence, of $T - T_c$). When plotted, one indeed can see the perfect data collapse for different values of ξ, which is the first nontrivial test of the quality of our results for the scaling function.

In Fig. 6, we plot the BMW scaling function together with the experimental results from Ref. [49]. Due to the small values taken by the coefficients c_n and the critical exponent η in $d = 3$, the Ornstein-Zernicke behavior dominates even beyond $p\xi = 1$. In order to measure the deviation from this behavior, one usually makes use of the auxiliary function,

$$h(x) = \ln\left[\frac{g(x)}{g_{OZ}(x)}\right]. \tag{55}$$

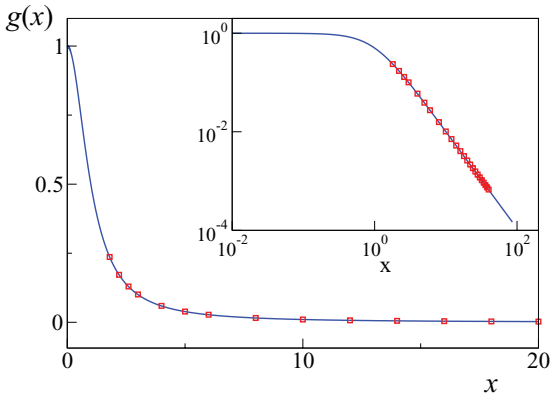

FIG. 6. (Color online) The two-point scaling function $g(p\xi)$ as a function of $x = p\xi$ in the high-temperature phase ($d = 3$, $N = 1$). Solid blue line, BMW result. Red squares, experimental results of Ref. [49]. Inset, same data with logarithmic scales.

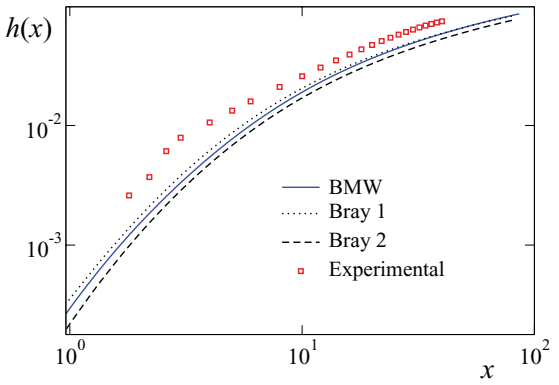

FIG. 7. (Color online) Deviation in the scaling function from its trivial Ornstein-Zernicke form, Eq. (55). The dotted and dashed lines correspond to two extreme choices of parameters C_2 and C_3 of Bray's ansatz. Dotted line, $C_1 = 0.924$, $C_2 = 1.8$, and $C_3 = -2.28$. Dashed line, $C_1 = 0.918$, $C_2 = 2.55$, and $C_3 = -3.45$.

In Fig. 7, we plot this function together with the experimental results from Ref. [49] and the results from the Bray ansatz for two extreme choices of the C_2^+ and C_3^+ parameters. There, one can see that the BMW approximated result compares very well with all these results. In particular, it is in between the results obtained from the two Bray ansätze considered.

Let us mention that, even with large system sizes, the MC results suffer from significant systematic errors for $p\xi$ larger than typically 5–10. This probably comes from the fact that the universal behavior of the structure factor shows up only when ξ and separation l between the spins, at which we calculate the correlation function, are large compared to the lattice spacing and are small compared to the lattice size: Even for lattice sizes of a few hundreds of lattice spacings, this leaves only a small window of useful values of ξ/l [46].

On top of these results, we also can compare results for the values of coefficients c_2^+ and C_1^+. The results for BMW are $c_2^+ \sim -4.5 \times 10^{-4}$ to be compared with the improved high-temperature best estimate [51] $c_2^+ = -3.90(6) \times 10^{-4}$, whereas, for C_1^+, BMW yields $C_1^+ = 0.914$ to be compared with the ε-expansion result $C_1^+ = 0.92$.

We conclude this section by noting that (i) the structure factor encompasses much more information on the universal behavior of a model than the (leading) critical exponents (that, moreover, are difficult to measure experimentally), (ii) Bray's ansatz, although powerful, depends on two parameters C_2 and C_3 that perturbatively are determined poorly as well as on two critical exponents, (iii) the present state of the art of the MC simulations, by far, is insufficient to reliably compute the structure factor in the interesting region of momentum where $p\xi$ is large, and (iv) the BMW method leads to a determination of the structure factor that has no free parameter once a choice of regulator has been made (possibly involving an optimization procedure as described in Sec. V B). The results above, summarized in Fig. 7, suggest that the BMW method leads to an accurate determination of the structure factor in the whole momentum range, while the experimental results seem to suffer at small momentum from systematic deviations.

VII. RELATION WITH THE DERIVATIVE EXPANSION

The validity of the DE rarely is questioned, satisfactory results being taken as an *a posteriori* check. We now show that the BMW approach allows for a deeper understanding of its range of applicability and of some of its peculiar features.

The ansatz defining the order of the DE [see, for instance, Eq. (12) for order 2] is used to

(i) define the quantities to be determined, which, in the case of order 2, are the effective potential and the field normalization, both functions of the (constant) field ϕ,

$$V_k(\phi) = \frac{1}{\Omega}\Gamma_k[\phi(x)]|_{\phi(x)=\phi},$$
$$Z_k(\phi) = \partial_{p^2}\left(\Gamma_k^{(2)}[p;\phi]\right)\Big|_{p=0,\phi}. \tag{56}$$

(ii) Compute the n-point functions $\Gamma_k^{(n)}$ and the propagator $G_k = (\Gamma_k^{(2)} + R_k)^{-1}$ that enter the right hand sides of the flow equations of V_k, Z_k, etc.

In short, the DE projects the functional $\Gamma_k[\phi]$ on a polynomial expansion in powers of the derivatives of the field, the expansion coefficients being field dependent. In Fourier space, the DE amounts to a polynomial expansion of the n-point functions $\Gamma_k^{(n)}(p_1,\ldots,p_n;\phi)$ in powers of the momenta p_i around vanishing momenta [see, for instance, Eq. (18)]. At this point, it is useful to introduce a distinction between *external* momenta, the momenta that appear in the n-point function $\Gamma_k^{(n)}(p_1,\ldots,p_n;\phi)$ whose flow is being considered and the *internal* momentum, denoted by q, appearing in the n-point functions on the right hand side of the corresponding flow equation and which is integrated over. In contrast to what is performed in the BMW approximation, in the DE, no distinction is made between these two sets of momenta, which can lead to inconsistencies. For instance, in the flow equation for $Z_k(\phi)$ at order 2, the product $\Gamma_k^{(3)}(p,q,-p-q)\Gamma_k^{(3)}(-p,-q,p+q)$ [see Eq. (11)] leads to four terms of order 4: $(p^2)^2, p^2q^2, (pq)^2, (q^2)^2$, which, in a strict expansion to this order, should be neglected (notice that this usually is not what is performed in the context of the DE of Wetterich's equation). In fact, since $Z_k(\phi)$ already is the coefficient of the p^2 term in the expansion of $\Gamma_k^{(2)}(p;\phi)$, any dependence of $\Gamma_k^{(3)}$ (and of $\Gamma_k^{(4)}$) on the internal momentum q should be neglected in $\partial_k Z_k(\phi)$ at this order of the DE. Since the BMW approximation at order $s = 2$ precisely consists of setting $q = 0$ in $\Gamma_k^{(3)}$ and $\Gamma_k^{(4)}$ in the flow equation of $\Gamma_k^{(2)}$, we conclude that, at this order, the BMW approximation contains all terms of the DE at order ∇^2.

The BMW approximation, which disentangles the roles of the internal and external momenta, differs deeply from the DE precisely on the point explained above: As the DE, it takes advantage of the fact that the internal momentum is cut off by $\partial_k R_k(q)$ in order to expand in powers of q/k (in fact, only the leading term $q = 0$ is retained) but does not rely on the smallness of the external momenta.

In fact, the natural expansion parameter of the DE is the ratio p/k or p/m, whichever is smallest where m is the smallest of the masses that may appear in the problem considered: When k is much larger than all the masses, these can be ignored, and p/k is the expansion parameter. When k becomes smaller than the smallest mass, the flow essentially stops, and the expansion parameter becomes p/m in the limit $k \to 0$. Thus, it is plausible that the DE performed as a power series in p/k in a critical theory ($m = 0$) possesses a radius of convergence on the same order as the DE performed as a power series in p/m in a massive theory at $k = 0$. In this last case, the radius of convergence is known for $N = 1$ in dimension three [48,50]: It is three in the symmetric phase and two in the broken phase.[2]

The above arguments suggest that the DE is not able to describe k-dependent correlation functions with external momenta higher than typically $3\max(k,m)$. In particular, in the critical case where massless modes are present, the DE only is suited for the calculation of physical (that is, at $k = 0$) correlation functions at $p = 0$: The anomalous momentum behavior $\Gamma_{k=0}^{(2)}(p) \sim p^{2-\eta}$, valid at small p, will not emerge at any order of the DE. Of course, this does not mean that the anomalous dimension cannot be determined within the DE as one can exploit general scaling relations and the fact that the anomalous dimension also enters quantities that are defined *at* zero momentum. Thus, for instance, η can be estimated from the k dependence of the normalization factor $Z_k \sim k^{-\eta}$ (or, alternatively, from the large-field behavior of the fixed-point dimensionless effective potential). In contrast, the BMW approximation correctly captures the anomalous scaling of $\Gamma_{k=0}^{(2)}(p)$ at small p, and this is a direct consequence of the fact that no expansion in external momenta is performed.[3]

The origin of the difficulties of the DE is that it does not have good decoupling properties in the momentum range $p \gg k$. The decoupling property, crucial for universality, means, on the example on the two-point function, that $\Gamma_k^{(2)}(p)$ becomes almost k independent when $k \ll p$ and that, therefore, $\Gamma_{k=0}^{(2)}(p) \simeq \Gamma_{k=p}^{(2)}(p)$. Thus, one naively could expect that external momenta $\{p_i\}$, $i = 1,\ldots,n$ play the role of IR regulators in the flow of $\Gamma_k^{(n)}(\{p_i\})$ and that, when $k < p_i$, $\forall\, i$, the flow of $\Gamma_k^{(n)}$ (almost) stops. In fact, in flow equations, external momenta play, at best, the role of IR regulators when all momenta involved (external and internal) are not in an exceptional configuration. The problem is that, even when the external momenta are not exceptional, the integral over the internal momentum q in the flow equation of $\Gamma_k^{(n)}$ involves vertex functions ($\Gamma_k^{(n+1)}$ or $\Gamma_k^{(n+2)}$) in exceptional configurations. Depending on the approximation scheme, this can spoil

[2]The reason is understood easily in the Minkowskian version of the theory. In this case, $3m$ is the particle production threshold (in the symmetric phase) that reflects itself as a pole in the complex-momentum plane. This pole, which is the closest to the origin, determines the radius of convergence of the expansion in powers of p. The same reasoning leads to $2m$ in the broken phase except if there exists a two-particle bound state, in which case, its mass (which is smaller than $2m$) determines the radius of convergence. It is very probable that such a bound state exists in the $d = 3$ and $N = 1$ cases [53], and its mass has been found on the order of $1.8m$. Note that this kind of analysis can be generalized for any model with a Minkowskian unitary extension.

[3]We recall that the two determinations of η performed within the BMW approximation, either through the momentum dependence of $\Gamma_{k=0}^{(2)}(p)$ or from Z_k, lead to the same values of this exponent.

the decoupling property that, undoubtly, should hold for the (physical, that is, $k \ll p$) correlation functions themselves when they are evaluated in nonexceptional configurations. Therefore, the difficulty is to devise an approximation scheme that satisfies the decoupling property. While this is the case for the BMW scheme, it is neither of the perturbation theory nor of the DE. Nevertheless, from the DE, one can try to extract, the gross behavior of $\Gamma^{(2)}(p)$ (and of the other functions) by stopping the flow at $k = p$ by hand and by identifying $\Gamma^{(2)}_{k=p}(p)$ with $\Gamma^{(2)}_{k=0}(p)$. This idea has been explored in Ref. [8] (see also Ref. [52]). The resulting correlation functions roughly show the expected momentum behavior, but as analyzed in detail in Ref. [8], it does not seem possible to extend this first qualitative analysis and to obtain quantitatively precise correlation functions without having recourse to BMW.

To gain further insight into the validity of the DE, we may consider a simple analytical representation of the function $\Gamma^{(2)}_{k=0}(p;\phi)$ determined with the BMW approximation at order $s = 2$, which, as we have shown, is very close to the exact two-point function over the whole momentum range. The following formula (inspired by Eq. (2.33) of Ref. [4]):

$$\Gamma^{(2)}_k(p,\rho) = Ap^2\left[p^2 + b\,k^2 + b' M_k^2(\rho)\right]^{-\eta_k/2} + V'_k + 2\rho V''_k \tag{57}$$

where A, b, and b' are independent of p and ρ and $M_k^2(\rho)$ is a function homogeneous to a square mass, provides a good fit for the BMW results when k as well as $M_k^2(\rho)$ are very small compared to the UV cutoff Λ. This formula encompasses the two different regimes that characterize the behavior of $\Gamma^{(2)}_k(p)$ at small p: First, for p, small compared to Λ, and large, compared to k and to the mass, it yields $\Gamma^{(2)}_k(p) \sim p^{2-\eta_k}$, with η_k as the running anomalous dimension. Thus, the critical behavior is captured for k sufficiently small for η_k to be quasistationary and (almost) equal to η. Second, for p, small compared to either M_k or k, one can expand $\Gamma^{(2)}_k(p;\phi)$ in powers of $p^2/(k^2 + M_k^2)$ and can get

$$\Gamma^{(2)}_k(p,\rho) = A'\left[k^2 + b''\,M_k^2(\rho)\right]^{-\eta_k/2} p^2[1 + f_{1,k}(\rho)p^2 + f_{2,k}(\rho)p^4 + \cdots] + V'_k + 2\rho V''_k. \tag{58}$$

This is the kind of ansatz considered by the DE, and it illustrates how the anomalous dimension can be extracted from the k dependence of the coefficient of the p^2 term in the running action [8].

Finally, let us stress that the above remarks, while they provide some justification for the DE and, in particular, specify the conditions for its validity, are not sufficient to prove convergence, which may strongly be affected by the regulator. In particular, one may expect systematic errors in cases where the range of the cutoff function $R_k(q)$ is not smaller than the natural radius of convergence of the DE. Notice, however, that, at least for $N = 1$ in $d = 3$, the smallness of the c_n coefficients in Eq. (48) suggest that, even at low order, the DE should be able to capture the low-momentum physics. An in-depth study of this issue will be presented in Ref. [22].

VIII. CONCLUSIONS

In this paper, we have presented the complete numerical implementation of the BMW approximation scheme that allows for a solution of the NPRG flow equations, keeping the full-momentum dependence of the two-point function. At the level considered in this paper, this amounts to solving two coupled equations for the effective potential and the two-point function. These equations can be solved by elementary numerical techniques.

We have considered applications to the $O(N)$ models, mostly in dimension $d = 3$. An accurate momentum dependence of the two-point function has been obtained from the low-momentum critical region to the high-momentum perturbative region (such a region exists when the dimensionful bare coupling is small compared to the UV cutoff). In particular, the critical exponents are determined accurately as already reported in Ref. [12]. The additional results presented in this paper concern the scaling functions that probe a different aspect of the momentum dependence of the two-point function in the vicinity of the critical point. More specifically, we have considered the scaling function for the case $N = 1$ above the critical point and have shown that it is in excellent agreement with the best available theoretical estimates. Interestingly, these estimates, including ours, differ significantly from the experimental data at small momenta. These scaling functions, which are difficult to obtain with other more conventional techniques, including MC simulations, come out directly from the two-point function obtained by solving the flow equations.

Another piece of information of physical interest, which also was contained in the two-point function that we computed, was its field dependence. Thus, a natural application of the present method could be the investigation of the $O(N)$ models in the presence of an external magnetic field. We also could contemplate extracting information about possible bound states from the two-point function [53]. Finally, we note that the BMW method paves the way toward understanding a variety of situations where the momentum structure plays a crucial role. For instance, a method similar in spirit has been applied successfully to the determination of the fixed-point structure of the Kardar-Parisi-Zhang equation [54,55] and to the calculation of the spectral function in a Bose gas [52].

ACKNOWLEDGMENT

We thank N. Dupuis for discussions and remarks on the first version of the paper.

APPENDIX A: NOTATION AND CONVENTIONS

By taking successive functional derivatives of $\Gamma_k[\phi]$ with respect to $\phi(x)$ and then letting the field be constant, one gets the n-point functions,

$$\Gamma^{(n)}_k(x_1,\ldots,x_n;\phi) \equiv \left.\frac{\delta^n \Gamma_k}{\delta\phi(x_1)\cdots\delta\phi(x_n)}\right|_{\phi(x)\equiv\phi}, \tag{A1}$$

in a constant background field ϕ. Since the background is constant, these functions are invariant under translations of the coordinates, and it is convenient to factor the δ function that expresses the conservation of the total momentum out of the

definition of their Fourier transform. Thus, with the usual abuse of notation, we define the n-point functions $\Gamma_k^{(n)}(p_1,\ldots,p_n;\phi)$ as

$$(2\pi)^d\delta^{(d)}\Big(\sum_j p_j\Big)\Gamma_k^{(n)}(p_1,\ldots,p_n;\phi) \equiv \int d^dx_1\cdots d^dx_n e^{i\sum_j p_j x_j}\Gamma_k^{(n)}(x_1,\ldots,x_n;\phi).$$

Here, we use the convention of incoming momenta, and it is understood that, in $\Gamma_k^{(n)}(p_1,\ldots,p_n;\phi)$, the sum of all momenta vanishes so that $\Gamma_k^{(n)}$ is actually a function of $n-1$ momentum variables (and of ϕ). Notice that we use brackets for the functional, e.g., $\Gamma_k[\phi]$ and parentheses for functions, e.g., $\Gamma_k^{(n)}(p_1,\ldots,p_n;\phi)$ when ϕ is uniform. For the two-point function evaluated in a uniform-field configuration, which effectively depends on a single momentum p, we often use the simplified notation $\Gamma_k^{(2)}(p;\phi)$ in place of $\Gamma_k^{(2)}(p,-p;\phi)$.

APPENDIX B: EXTENSION OF BMW

In the approximation BMW with $s=2$, we make the following substitutions on the right hand side of the flow equation for $\Gamma_k^{(2)}(p)$: $\Gamma_k^{(4)}(p,-p,q,-q)\longrightarrow\Gamma_k^{(4)}(p,-p,0,0)$ and $\Gamma_k^{(3)}(p,q,-p-q)\longrightarrow\Gamma_k^{(3)}(p,0,-p)$, that is, we set the loop momentum q to zero in the three- and four-point functions. (In this Appendix, we explicitly do not indicate the dependence on ϕ for all n-point functions in order to alleviate the notation.) By doing so, one obtains a closed equation for the two-point function $\Gamma_k^{(2)}(p)$, which is the object calculated with optimum accuracy at the level $s=2$. As explained in the main part of the paper, the general strategy to obtain the three- and four-point functions with comparable accuracy is to consider higher orders ($s>2$) in the approximation scheme. However, in this appendix, we show that one already can improve the accuracy of $\Gamma_k^{(3)}$ and $\Gamma_k^{(4)}$ simply by exploiting the information available on $\Gamma_k^{(2)}(p)$.

First, let us consider the function $\Gamma_k^{(4)}$. We know that, at one loop and in vanishing fields, it has the following structure:

$$\Gamma_k^{(4),\,\text{one loop}}(p_1,p_2,p_3,p_4) = f(p_1+p_2)+f(p_1+p_3)+f(p_1+p_4), \quad \text{(B1)}$$

where the function $f(p)$ is found easily to be

$$f(p)=\tfrac{1}{2}\Gamma_k^{(4)}(p,-p,0,0)-\tfrac{1}{6}\Gamma_k^{(4)}(0,0,0,0). \quad \text{(B2)}$$

Since $\Gamma_k^{(4)}(p,-p,0,0)=\partial_\phi^2\Gamma_k^{(2)}(p)$ (for the constant field ϕ), we arrive at the following expression for the four-point function in terms of the two-point function $\Gamma_k^{(2)}(p)$:

$$\Gamma_k^{(4)}(p_1,p_2,p_3,p_4)\approx\tfrac{1}{2}\partial_\phi^2\Gamma_k^{(2)}(p_1+p_2)+\tfrac{1}{2}\partial_\phi^2\Gamma_k^{(2)}(p_1+p_3)+\tfrac{1}{2}\partial_\phi^2\Gamma_k^{(2)}(p_1+p_4)-\tfrac{1}{2}\partial_\phi^2\Gamma_k^{(2)}(0). \quad \text{(B3)}$$

Note that, by construction, this expression is symmetric under the exchange of the external legs, and it is one-loop exact at zero external field.

For the function $\Gamma_k^{(3)}$, one can extract the following equivalent in the limit of a vanishing field:

$$\frac{\Gamma_k^{(3)}(p,q,l)}{\phi}\sim\partial_\phi\Gamma_k^{(3)}(p,q,l)\Big|_{\phi=0} \sim\Gamma_k^{(4)}(p,q,l,0)|_{\phi=0}\,. \quad \text{(B4)}$$

Then, by using the approximation above for $\Gamma_k^{(4)}$ (B3), one obtains the following expression for $\Gamma_k^{(3)}$, whose zero field equivalent is exact at one loop:

$$\Gamma_k^{(3)}(p,q,l)\approx\tfrac{1}{2}\partial_\phi\Gamma_k^{(2)}(p)+\tfrac{1}{2}\partial_\phi\Gamma_k^{(2)}(q)+\tfrac{1}{2}\partial_\phi\Gamma_k^{(2)}(l)-\tfrac{1}{2}\partial_\phi\Gamma_k^{(2)}(0). \quad \text{(B5)}$$

At this point, we note that we may use the new expressions that we have obtained for $\Gamma_k^{(3)}$ and $\Gamma_k^{(4)}$ in the flow equation for $\Gamma_k^{(2)}$. Since these n-point functions are now one-loop exact, the resulting approximation for $\Gamma_k^{(2)}$ will be two-loop exact in a zero external field. Therefore, this yields an improvement of the BMW approximation, in particular, in the high-momentum region where we know that it loses accuracy.

Consider then Eq. (11) for $\Gamma_k^{(2)}$, and rewrite it in terms of $\Delta_k(p)$,

$$\partial_t\Delta_k(p;\rho)=\int_q\partial_t R_k(q)G_k^2(q)\Big\{\big[\Gamma_k^{(3)}(p,q,-p-q)\big]^2\times G_k(q+p)-\big[\Gamma_k^{(3)}(0,q,-q)\big]^2G_k(q)-\frac{1}{2}\big[\Gamma_k^{(4)}(p,-p,q,-q)-\Gamma_k^{(4)}(0,0,q,-q)\big]\Big\}. \quad \text{(B6)}$$

Next, perform the substitutions (B5), and

$$\Gamma_k^{(4)}(p,-p,q,-q)\to\tfrac{1}{2}\partial_\phi^2\Gamma_k^{(2)}(p+q,-p-q)+\tfrac{1}{2}\partial_\phi^2\Gamma_k^{(2)}(p-q,-p+q). \quad \text{(B7)}$$

One then gets

$$\partial_t\Delta_k(p)=2\rho H(p)-\tfrac{1}{2}L(p), \quad \text{(B8)}$$

with

$$H(p)\equiv\int_q\partial_t R_k(q)G_k^2(q)\Big\{G_k(q+p)\Big[\frac{1}{2}\Delta_k'(p)+\frac{1}{2}\Delta_k'(q)+\frac{1}{2}\Delta_k'(p+q)+3V_k''+2\rho V_k'''\Big]^2-G_k(q)[\Delta_k'(q)+3V_k''+2\rho V_k''']^2\Big\}, \quad \text{(B9)}$$

and

$$L(p)=\int_q\partial_t R_k(q)\,G_k^2(q)\{\Delta_k'(p+q)+2\rho\Delta_k''(p+q)-\Delta_k'(q)-2\rho\Delta_k''(q)\}. \quad \text{(B10)}$$

It is not difficult to generalize these expressions for the $O(N)$ model with arbitrary N. However, we do not present these here because, despite the good properties presented above, this extended version of the BMW approximation proves to be unstable numerically, and we have not been able to solve the

corresponding equations with simple techniques. A further analysis, using more elaborate numerical techniques, is called for.

APPENDIX C: INTEGRALS

In this Appendix, we give details on the calculation of the integrals $I_n(k;\rho)$ and $J_n(p;k;\rho)$.

In the case of integral $I_n(k;\rho)$, since $G_k(q)$ (in a uniform external field) depends only on q^2, the angular integral is straightforward. One gets

$$I_n = \frac{S_d}{(2\pi)^d}\int_0^\infty dq\, q^{d-1}\partial_t R_k(q) G_k^n(q;\rho), \tag{C1}$$

where

$$S_d = \frac{2\pi^{d/2}}{\Gamma(d/2)}, \quad K_d = \frac{S_d}{d(2\pi)^d}. \tag{C2}$$

In the case of integral $J_n(p;k;\rho)$, the presence of the external momentum p makes the angular integral more involved.

1. Angular integrations

Consider integrals generically of the form

$$\int_q F(|p+q|) \equiv \mathcal{I}(p). \tag{C3}$$

One can proceed as follows:

$$\begin{aligned}\mathcal{I}(p) &= \int_q g(q)F(|p+q|)\\ &= \int_0^\infty dq\, q^{d-1} g(q)\int \frac{d\Omega_d}{(2\pi)^d} F(|p+q|)\\ &= \frac{S_{d-1}}{(2\pi)^d}\int_0^\infty dq\, q^{d-1} g(q)\\ &\quad\times \int_0^\pi d\theta\, \sin^{d-2}\theta\, F(\sqrt{p^2+q^2+2pq\,\cos\theta})\\ &= \frac{S_{d-1}}{(2\pi)^d}\int_0^\infty dq\, q^{d-2}\,\frac{g(q)}{p}\\ &\quad\times \int_{|p-q|}^{p+q} d\xi\, \xi\, \mathcal{J}_d(\xi,p,q) F(\xi),\end{aligned} \tag{C4}$$

where we made a change in variables $\xi \equiv \sqrt{p^2+q^2+2pq\,\cos\theta}$, and

$$\mathcal{J}_d(\xi,p,q) \equiv \left[1-\left(\frac{\xi^2-p^2-q^2}{2pq}\right)^2\right]^{(d-3)/2}. \tag{C5}$$

The interest in the last formula (C4) lies in the fact that the needed integration points belong to the grid so that the integral can be calculated numerically without the need for interpolation. Furthermore, this method is particularly convenient in $d=3$ because the Jacobian (C5) then is trivial.

2. Dimensions less than 3

The Jacobian (C5) is unity in $d=3$ and is regular for $d>3$ but becomes singular for $d<3$. More precisely, for $d<3$, it diverges when ξ approaches the boundaries of its integration domain ($\xi = p+q$ or $|p-q|$). Even if the integral eventually converges, this divergence is the source of numerical difficulties.

For $d<3$, we then use a different strategy based on Cartesian variables. We define q_1 as the component of q along p and proceed as follows:

$$\begin{aligned}\mathcal{I}(p) &= \int \frac{d^{d-1}q_2}{(2\pi)^{d-1}}\int_{-\infty}^{+\infty}\frac{dq_1}{2\pi} g(q)F(|p+q|)\\ &= \frac{S_{d-1}}{(2\pi)^d}\int_0^\infty q_2^{d-2}dq_2\\ &\quad\times\int_{-\infty}^\infty dq_1, g(q)F\left(\sqrt{p^2+q_1^2+q_2^2+2pq_1}\right),\end{aligned} \tag{C6}$$

with q as the modulus of the vector $\mathbf{q}$: $q=\sqrt{q_1^2+q_2^2}$ and $|p+q| = \sqrt{p^2+q_1^2+q_2^2+2pq_1}$.

This expression has no singularities for $d \geqslant 2$, but it requires multiple interpolations that make the numerics more involved than in $d \geqslant 3$.

3. Small-momentum limits

Integral $J_n(p;k;\rho)$ is regular when $p\to 0$. However, the expression given by the angular integration does not make this manifest. To get the small p behavior of the generic integral (C3), one directly can expand $F(|\mathbf{p}+\mathbf{q}|)-F(q)$ in the first line of Eq. (C4),

$$\begin{aligned}F(|\mathbf{p}+\mathbf{q}|)-F(q) &= \frac{2\mathbf{p}\cdot\mathbf{q}+p^2}{2q}\partial_q F(q)\\ &\quad+\frac{(\mathbf{p}\cdot\mathbf{q})^2}{2q^2}\left[\partial_q^2 F(q)-\frac{1}{q}\partial_q F(q)\right]\\ &\quad+O(p^3).\end{aligned} \tag{C7}$$

Then, one can use, with the brackets denoting angular averages,

$$\begin{aligned}\langle f(q)\rangle &= \frac{1}{S_d}\int d\Omega_d\,(q) = f(q),\\ \langle(\mathbf{q}\cdot\mathbf{p})\, f(q)\rangle &= \frac{1}{S_d}\int d\Omega_d(\mathbf{q}\cdot\mathbf{p}) f(q) = 0,\\ \langle(\mathbf{q}\cdot\mathbf{p})^2 f(q)\rangle &= \frac{1}{S_d}\int d\Omega_d(\mathbf{q}\cdot\mathbf{p})^2 f(q)\\ &= \frac{p^2q^2}{d} f(q)\end{aligned} \tag{C8}$$

to obtain

$$\begin{aligned}&\langle F(|\mathbf{p}+\mathbf{q}|)-F(q)\rangle\\ &\quad= \frac{p^2}{2d}\left[\partial_q^2 F(q)+\frac{d-1}{q}\partial_q F(q)\right]+O(p^4),\end{aligned} \tag{C9}$$

and

$$\begin{aligned}\mathcal{I}(p)-\mathcal{I}(0) &= \frac{p^2}{2}K_d\int_0^\infty dq\, g(q) q^{d-1}\\ &\quad\times\left[\partial_q^2 F(q)+\frac{d-1}{q}\partial_q F(q)\right]+O(p^4)\\ &= \frac{p^2}{2}K_d\int_0^\infty dq\, g(q)\partial_q[q^{d-1}\partial_q F(q)]+O(p^4).\end{aligned} \tag{C10}$$

APPENDIX D: GENERALIZATION FOR $O(N)$ MODELS

In this Appendix, the $s = 2$ BMW approximation and the corresponding flow equations are presented for $O(N)$ models. The exact flow of the two-point function in a constant external field reads (we omit the renormalization group parameter k in this appendix for notational simplicity)

$$\begin{aligned}\partial_t \Gamma^{(2)}_{ab}(p,\boldsymbol{\phi}) &= \int_q \partial_t [R(q)]_{in} \Big\{ G_{ij}(q,\boldsymbol{\phi}) \Gamma^{(3)}_{ajh}(p,q,-p-q,\boldsymbol{\phi}) G_{hl} \\ &\quad \times (q+p,\boldsymbol{\phi}) \Gamma^{(3)}_{blm}(-p,p+q,-q,\boldsymbol{\phi}) G_{mn}(q,\boldsymbol{\phi}) \\ &\quad - \frac{1}{2} G_{ij}(q,\boldsymbol{\phi}) \Gamma^{(4)}_{abjh}(p,-p,q,-q,\boldsymbol{\phi}) G_{hn}(q,\boldsymbol{\phi}) \Big\},\end{aligned} \tag{D1}$$

where $a,b,\ldots$ denote $O(N)$ indices and $\boldsymbol{\phi}$ denotes an N-component uniform field. Within the BMW approximation, we perform the substitutions,

$$\begin{aligned}\Gamma^{(3)}_{ajh}(p,q,-p-q,\boldsymbol{\phi}) &\to \frac{\partial \Gamma^{(2)}_{ah}(p,-p,\boldsymbol{\phi})}{\partial \phi_j}, \\ \Gamma^{(4)}_{abjh}(p,-p,q,-q,\boldsymbol{\phi}) &\to \frac{\partial^2 \Gamma^{(2)}_{ab}(p,-p,\boldsymbol{\phi})}{\partial \phi_j \partial \phi_h}.\end{aligned} \tag{D2}$$

In order to manifestly preserve the $O(N)$ symmetry along the flow, the regulator ΔS_k has to be an $O(N)$ scalar, and, accordingly, the cutoff function has to be a tensor,

$$[R(q)]_{ij} \equiv R(q)\delta_{ij}.$$

The symmetry of the theory also implies that the matrix of the two-point functions can be written in terms of two independent tensors. We chose to write it in the form

$$\Gamma^{(2)}_{ab}(p,-p,\boldsymbol{\phi}) = \Gamma_A(p,\rho)\delta_{ab} + \phi_a\phi_b \Gamma_B(p,\rho), \tag{D3}$$

with $\rho = \frac{1}{2}\sum_a \phi_a\phi_a$. This form turns out to be convenient in the limit $\rho \to 0$.

The symmetry also allows us to write the propagator in this equation in terms of its longitudinal and transverse components with respect to the external field,

$$\begin{aligned}G_{ab}(p^2,\boldsymbol{\phi}) &= G_T(p^2,\rho)\left(\delta_{ab} - \frac{\phi_a\phi_b}{2\rho}\right) \\ &\quad + G_L(p^2,\rho)\frac{\phi_a\phi_b}{2\rho}.\end{aligned} \tag{D4}$$

It is easy to find the relationship between these propagators and Γ_A and Γ_B,

$$G_T^{-1}(p,\rho) = \Gamma_A(p,\rho) + R(p), \tag{D5}$$

$$G_L^{-1}(p,\rho) = \Gamma_A(p,\rho) + 2\rho\Gamma_B(p,\rho) + R(p). \tag{D6}$$

Using the definition (D3) of the functions Γ_A and Γ_B as well as the form given above for the propagators, one can decompose the flow equation (D1) in two equations for Γ_A and Γ_B.

As in the case of $N = 1$, we introduce the functions,

$$\Delta_A(p,\rho) = \Gamma_A(p,\rho) - p^2 - \Gamma_A(p=0,\rho), \tag{D7}$$

$$\Delta_B(p,\rho) = \Gamma_B(p,\rho) - \Gamma_B(p=0,\rho). \tag{D8}$$

Notice that, at the bare level, $\Gamma_A(p,\rho) - \Gamma_A(p=0,\rho) = p^2$ while $\Gamma_B(p,\rho) - \Gamma_B(p=0,\rho) = 0$, which explains the difference between the two definitions. In terms of these functions, Γ_A and Γ_B read

$$\Gamma_A(p,\rho) = p^2 + \Delta_A(p,\rho) + V', \tag{D9}$$

$$\Gamma_B(p,\rho) = \Delta_B(p,\rho) + V'', \tag{D10}$$

where the primes denote derivatives with respect to ρ. The equations for Δ_A and Δ_B read

$$\partial_t \Delta_A(p,\rho) = 2\rho\left\{J_3^{LT}(\Delta_A' + V'')^2 + J_3^{TL}(\Delta_B + V'')^2 - \left(I_3^{LT} + I_3^{TL}\right)V''^2\right\} - \tfrac{1}{2} I_2^{LL}(\Delta_A' + 2\rho\Delta_A'') - \tfrac{1}{2} I_2^{TT}[(N-1)\Delta_A' + 2\Delta_B], \tag{D11}$$

$$\begin{aligned}\partial_t \Delta_B(p,\rho) &= J_3^{TT}(N-1)(\Delta_B + V'')^2 - J_3^{LT}(\Delta_A' + V'')^2 - J_3^{TL}(\Delta_B + V'')^2 + J_3^{LL}\{(\Delta_A' + 2\Delta_B + 3V'')^2 \\ &\quad + 4\rho(\Delta_B' + V''')(\Delta_A' + 2\Delta_B + 3V'') + 4\rho^2(\Delta_B' + V''')^2\} - \tfrac{1}{2} I_2^{TT}(N-1)\Delta_B' - \tfrac{1}{2} I_2^{LL}(5\Delta_B' + 2\rho\Delta_B'') \\ &\quad - \left[(N-1)I_3^{TT} - I_3^{LT} - I_3^{TL}\right]V''^2 - I_3^{LL}(3V'' + 2\rho V''')^2 + \Delta_B I_A - \left\{(N-1)I_3^{TL} - I_3^{LT} - I_3^{TL}\right\}V''^2,\end{aligned} \tag{D12}$$

where we have omitted the ρ and p dependences on the right hand side for compactness. We have introduced the integrals ($n > 1$),

$$\begin{aligned}J_n^{\alpha\beta}(p,\rho) &= \int_q \partial_t R(q) G_\alpha^{n-1}(q,\rho) G_\beta(p+q,\rho), \\ I_n^{\alpha\beta}(\rho) &= J_n^{\alpha\beta}(p=0,\rho),\end{aligned} \tag{D13}$$

with α, β standing either for L (longitudinal) or for T (transversal). For $n = 1$, we set

$$I_1 = (N-1)I_1^{TT}(\rho) + I_1^{LL}(\rho). \tag{D14}$$

It turns out to be useful to also introduce the integral,

$$I_A(\rho) \equiv \int_q \partial_t R(q)[G_L(q,\rho) + G_T(q,\rho)]G_L(q,\rho)G_T(q,\rho),$$

and, in intermediate steps, we have used the identity,

$$\frac{1}{\rho}\left[G_T^2(q,\rho) - G_L^2(q,\rho)\right] = 2G_L(q,\rho)G_T(q,\rho)\Gamma_B(q,\rho)[G_L(q,\rho) + G_T(q,\rho)], \tag{D15}$$

which allows us to handle expressions that manifestly are regular for $\rho = 0$.

As mentioned in the main text, an accurate study of the critical regime requires using dimensionless variables. Again, using $W(\rho) = V'(\rho)$, we define

$$k^2 Z_k[\tilde{p}^2 + \tilde{\Delta}_A(\tilde{\rho},\tilde{\rho})] = p^2 + \Delta_A(p,\rho), \tag{D16}$$

$$\tilde{\Delta}_B(\tilde{p},\tilde{\rho}) = \frac{K_d \Delta_B(p,\rho)}{Z_k^2 k^{4-d}}. \tag{D17}$$

We also have to use the dimensionless functions corresponding to Eq. (D13),

$$\tilde{I}_3^{\alpha\beta}(\tilde{\rho}) = I_3^{\alpha\beta}(\rho)\frac{Z_k^2 k^{4-d}}{K_d}, \quad \tilde{J}_3^{\alpha\beta}(\tilde{p},\tilde{\rho}) = J_3^{\alpha\beta}(p,\rho)\frac{Z_k^2 k^{4-d}}{K_d}, \quad \tilde{I}_2^{\alpha\beta}(\tilde{\rho}) = I_2^{\alpha\beta}(\rho)\frac{Z_k k^{2-d}}{K_d}. \tag{D18}$$

For numerical reasons, as explained in the main text for the $N = 1$ case, we study the flow of

$$\tilde{Y}_A(\tilde{p},\tilde{\rho}) = \frac{\tilde{\Delta}_A}{\tilde{p}^2}, \quad \tilde{Y}_B(\tilde{p},\tilde{\rho}) = \frac{\tilde{\Delta}_B}{\tilde{p}^2}. \tag{D19}$$

Then, the dimensionless flow equations can be calculated from Eqs. (D11) and (D12),

$$\partial_t \tilde{Y}_A(\tilde{p},\tilde{\rho}) = \eta\tilde{Y}_A + 1 + \tilde{p}\frac{\partial \tilde{Y}_A}{\partial \tilde{p}} + (d-2+\eta)\tilde{\rho}\tilde{Y}_A' + 2\tilde{\rho}\left\{\tilde{J}_3^{LT}\tilde{p}^2\left(\tilde{Y}_A' + \frac{\tilde{W}'}{\tilde{p}^2}\right)^2 + \tilde{J}_3^{TL}\tilde{p}^2\left(\tilde{Y}_B + \frac{\tilde{W}'}{\tilde{p}^2}\right)^2 - (\tilde{I}_3^{LT} + \tilde{I}_3^{TL})\frac{\tilde{W}'^2}{\tilde{p}^2}\right\}$$
$$- \frac{1}{2}\tilde{I}_2^{LL}(\tilde{Y}_A' + 2\tilde{\rho}\tilde{Y}_A'') - \frac{1}{2}\tilde{I}_2^{TT}[(N-1)\tilde{Y}_A' + 2\tilde{Y}_B], \tag{D20}$$

$$\partial_t \tilde{Y}_B(\tilde{p},\tilde{\rho}) = (d-2+2\eta)\tilde{Y}_B + \tilde{p}\frac{\partial \tilde{Y}_B}{\partial \tilde{p}} + (d-2+\eta)\tilde{\rho}\tilde{Y}_B' + (N-1)\tilde{J}_3^{TT}\tilde{p}^2\left(\tilde{Y}_B + \frac{\tilde{W}'}{\tilde{p}^2}\right)^2 + \tilde{J}_3^{LL}\left\{\tilde{p}^2\left(\tilde{Y}_A' + 2\tilde{Y}_B + \frac{3\tilde{W}'}{\tilde{p}^2}\right)^2\right.$$
$$\left. + 4\tilde{\rho}\tilde{p}^2\left(\tilde{Y}_A' + 2\tilde{Y}_B'\frac{3\tilde{W}}{\tilde{p}^2}\right)\left(\tilde{Y}_B' + \frac{\tilde{W}''}{\tilde{p}^2}\right) + 4\tilde{\rho}^2\tilde{p}^2\left(\tilde{Y}_B' + \frac{\tilde{W}''}{\tilde{p}^2}\right)^2\right\}$$
$$- \tilde{J}_3^{LT}\tilde{p}^2\left(\tilde{Y}_A' + \frac{\tilde{W}'}{\tilde{p}^2}\right)^2 - \tilde{J}_3^{TL}\left(\tilde{p}^2\tilde{Y}_B^2 + 2\tilde{Y}_B\tilde{W}' + \frac{\tilde{W}'^2}{\tilde{p}^2}\right) - \frac{\tilde{I}_3^{LL}}{\tilde{p}^2}(3\tilde{W}' + 2\tilde{\rho}\tilde{W}'')^2$$
$$- \left[(N-1)\tilde{I}_3^{TT} - \tilde{I}_3^{LT} - \tilde{I}_3^{TL}\right]\frac{\tilde{W}'^2}{\tilde{p}^2} - \frac{1}{2}\tilde{I}_2^{TT}(N-1)\tilde{Y}_B' - \frac{1}{2}\tilde{I}_2^{LL}(5\tilde{Y}_B' + 2\tilde{\rho}\tilde{Y}_B'') + \tilde{Y}_B I_A, \tag{D21}$$

with the primes now denoting derivatives with respect to $\tilde{\rho}$, and we have omitted the $\tilde{\rho}$ and $\tilde{p}$ dependences on the right hand side for compactness.

The flow equation for the potential, which reads

$$\partial_t V(\rho) = \tfrac{1}{2} I_1(\rho) \tag{D22}$$

allows us to derive an equation for the dimensionless derivative of the potential,

$$\partial_t \tilde{W}(\tilde{\rho}) = -(2-\eta)\tilde{W} + (d-2+\eta)\tilde{\rho}\tilde{W}' + \frac{1}{2}\frac{\partial \tilde{I}_1(\tilde{\rho})}{\partial \tilde{\rho}}. \tag{D23}$$

The flow of η_k follows from fixing a renormalization condition analogous to Eq. (36). For all values of k, we impose

$$\tilde{Y}_A(\tilde{p}_0,\tilde{\rho}_0) = 0. \tag{D24}$$

The simplest choice is $\tilde{p}_0 = 0$ and $\tilde{\rho}_0 = 0$. It leads to

$$\eta_k = \tfrac{1}{2}[N\tilde{Y}_A'(0,0) + 2\tilde{Y}_B(0,0)]\tilde{I}_2^{TT}(\tilde{\rho} = 0), \tag{D25}$$

where we have used $\tilde{I}_2^{TT}(\tilde{\rho} = 0) = \tilde{I}_2^{LL}(\tilde{\rho} = 0)$.

In the case of a generic renormalization point, the equation for η_k is more cumbersome,

$$\eta_k = \frac{-1}{1+\tilde{\rho}_0\tilde{Y}'_A}\left\{\tilde{p}_0\frac{\partial\tilde{Y}_A}{\partial\tilde{p}} + (d-2)\tilde{\rho}_0\tilde{Y}'_A + 2\tilde{\rho}_0\left[\tilde{J}_3^{LT}\left(\tilde{p_0}^2\tilde{Y}'^2_A + 2\tilde{Y}'_A\tilde{W}' + \frac{\tilde{W}'^2}{\tilde{p_0}^2}\right) - \tilde{I}_3^{LT}\frac{\tilde{W}'^2}{\tilde{p_0}^2}\right]\right.$$
$$\left. + 2\tilde{\rho}_0\left[\tilde{J}_3^{TL}\left(\tilde{p_0}^2\tilde{Y}_B^2 + 2\tilde{Y}_B\tilde{W}' + \frac{\tilde{W}'^2}{\tilde{p_0}^2}\right) - \tilde{I}_3^{TL}\frac{\tilde{W}'^2}{\tilde{p_0}^2}\right] - \frac{1}{2}\tilde{I}_2^{LL}(\tilde{Y}'_A + 2\tilde{\rho}_0\tilde{Y}''_A) - \frac{1}{2}\tilde{I}_2^{TT}[(N-1)\tilde{Y}'_A + 2\tilde{Y}_B]\right\}, \quad \text{(D26)}$$

with all functions evaluated at $\tilde{p} = \tilde{p}_0$ and $\tilde{\rho} = \tilde{\rho}_0$.

We also define

$$r_t(\tilde{q}) = -\eta\tilde{q}^2 r(\tilde{q}) - \tilde{q}^3\partial_{\tilde{q}} r(\tilde{q}), \quad \text{(D27)}$$

and the dimensionless propagators,

$$\tilde{G}_T(\tilde{p},\tilde{\rho}) = \frac{1}{\tilde{p}^2[\tilde{Y}_A + 1 + r(\tilde{p})] + \tilde{W}}, \quad \text{(D28)}$$

$$\tilde{G}_L(\tilde{p},\tilde{\rho}) = \frac{1}{\tilde{p}^2[\tilde{Y}_A + 1 + 2\tilde{\rho}\tilde{Y}_B + r(\tilde{p})] + \tilde{W} + 2\tilde{\rho}\tilde{W}'}, \quad \text{(D29)}$$

from which follow the expressions:

$$\tilde{I}_n^{\alpha\beta}(\tilde{\rho}) = d\int_0^\infty d\tilde{q}\,\tilde{q}^{d-1} r_t(\tilde{q})\tilde{G}_\alpha^{n-1}(\tilde{q})\tilde{G}_\beta(\tilde{q}), \quad \text{(D30)}$$

$$\tilde{J}_3^{\alpha\beta}(\tilde{p},\tilde{\rho}) = \frac{S_{d-1}}{K_d(2\pi)^d}\int_0^\infty d\tilde{q}\,\frac{\tilde{q}^{d-2}}{\tilde{p}} r_t(\tilde{q})\tilde{G}_\alpha^2(\tilde{q})\int_{|\tilde{p}-\tilde{q}|}^{\tilde{p}+\tilde{q}} d\xi\,\xi\,\mathcal{J}_d(\xi,\tilde{p},\tilde{q})\tilde{G}_\beta(\xi), \quad \text{(D31)}$$

with $\mathcal{J}_d(\xi,\tilde{p},\tilde{q})$ as defined in Eq. (C5). We also need the functions,

$$\tilde{I}_A(\tilde{\rho}) = \int_0^\infty d\tilde{q}\,\tilde{q}^{d-1}\{r_t(\tilde{q})[\tilde{G}_L(\tilde{q}) + \tilde{G}_T(\tilde{q})]\tilde{G}_L(\tilde{q})\tilde{G}_T(\tilde{q})[\tilde{Y}_B(\tilde{q})\tilde{q}^2 + \tilde{W}']\}, \quad \text{(D32)}$$

$$\tilde{K}^{\alpha\beta}(\tilde{\rho}) = \frac{1}{2dK_d}\frac{S_d}{(2\pi)^d}\int_0^\infty d\tilde{q}\,r_t(\tilde{q})\tilde{G}_\alpha(\tilde{q})\partial_{\tilde{q}}[\tilde{q}^{d-1}\partial_{\tilde{q}}\tilde{G}_\beta(\tilde{q})], \quad \text{(D33)}$$

that are used in the small-momentum region of the flow equations (cf. Appendix C in the $N = 1$ case).

[1] C. Wetterich, Phys. Lett. B **301**, 90 (1993).

[2] U. Ellwanger, Z. Phys. C **58**, 619 (1993); T. R. Morris, Int. J. Mod. Phys. A **9**, 2411 (1994).

[3] K. Wilson and J. Kogut, Phys. Rep. C **12**, 75 (1974); F. J. Wegner and A. Houghton, Phys. Rev. A **8**, 401 (1973); J. Polchinski, Nucl. Phys. B **231**, 269 (1984).

[4] J. Berges, N. Tetradis, and C. Wetterich, Phys. Rep. **363**, 223 (2002).

[5] M. Tissier, B. Delamotte, and D. Mouhanna, Phys. Rev. Lett. **84**, 5208 (2000); B. Delamotte, D. Mouhanna, and M. Tissier, Phys. Rev. B **69**, 134413 (2004); A. Sinner, N. Hasselmann, and P. Kopietz, Phys. Rev. Lett. **102**, 120601 (2009); Phys. Rev. A **82**, 063632 (2010); N. Dupuis, Phys. Rev. Lett. **102**, 190401 (2009); A. Rançon and N. Dupuis, Phys. Rev. B **83**, 172501 (2011); L. Canet, H. Chaté, B. Delamotte, I. Dornic, and M. A. Muñoz, Phys. Rev. Lett. **95**, 100601 (2005).

[6] S. Seide and C. Wetterich, Nucl. Phys. B **562**, 524 (1999); L. Canet, H. Chaté, and B. Delamotte, Phys. Rev. Lett. **92**, 255703 (2004); T. Machado and N. Dupuis, Phys. Rev. E **82**, 041128 (2010).

[7] J.-P. Blaizot, R. Mendéz-Galain, and N. Wschebor, Phys. Lett. B **632**, 571 (2006).

[8] J.-P. Blaizot, R. Mendéz-Galain, and N. Wschebor, Phys. Rev. E **74**, 051116 (2006); **74**, 051117 (2006).

[9] A. Parola and L. Reatto, Adv. Phys. **44**, 211 (1995); A. Parola, D. Pini, and L. Reatto, Phys. Rev. E **48**, 3321 (1993); Mol. Phys. **107**, 503 (2009).

[10] D. Guerra, R. Mendéz-Galain, and N. Wschebor, Eur. Phys. J. B **59**, 357 (2007).

[11] J.-P. Blaizot, R. Méndez-Galain, and N. Wschebor, Eur. Phys. J. B **58**, 297 (2007); F. Benitez, R. Méndez-Galain, and N. Wschebor, Phys. Rev. B **77**, 024431 (2008).

[12] F. Benitez, J.-P. Blaizot, H. Chaté, B. Delamotte, R. Méndez-Galain, and N. Wschebor, Phys. Rev. E **80**, 030103(R) (2009).

[13] N. Tetradis and C. Wetterich, Nucl. Phys. B **422**, 541 (1994).

[14] T. R. Morris, Int. J. Mod. Phys. A **9**, 2411 (1994).

[15] T. R. Morris, Phys. Lett. B **329**, 241 (1994).

[16] C. Bagnuls and C. Bervillier, Phys. Rep. **348**, 91 (2001).

[17] B. Delamotte, e-print arXiv:cond-mat/0702365.

[18] G. Tarjus and M. Tissier, Phys. Rev. Lett. **93**, 267008 (2004); M. Tissier and G. Tarjus, *ibid*. **96**, 087202 (2006); G. Tarjus and M. Tissier, Phys. Rev. B **78**, 024203 (2008); M. Tissier and G. Tarjus, *ibid*. **78**, 024204 (2008); J.-P. Kownacki and D. Mouhanna, Phys. Rev. E **79**, 040101 (2009); K. Essafi, J.-P. Kownacki, and D. Mouhanna, Phys. Rev. Lett. **106**, 128102 (2011); F. L. Braghin and N. Hasselmann, Phys. Rev. B **82**, 035407 (2010); N. Hasselmann and F. L. Braghin, Phys. Rev. E **83**, 031137 (2011); L. Canet, B. Delamotte, O. Deloubrière, and N. Wschebor, Phys. Rev. Lett. **92**, 195703 (2004); L. Canet, H. Chaté, B. Delamotte, and N. Wschebor, *ibid*. **104**, 150601 (2010).

[19] L. Canet, B. Delamotte, D. Mouhanna, and J. Vidal, Phys. Rev. D **67**, 065004 (2003); Phys. Rev. B **68**, 064421 (2003); L. Canet, *ibid*. **71**, 012418 (2005).

[20] C. Bagnuls and C. Bervillier, Condens. Matter Phys. **3**, 559 (2000).

[21] P. M. Stevenson, Phys. Rev. D **23**, 2916 (1981); T. L. Bell and K. G. Wilson, Phys. Rev. B **11**, 3431 (1975).

[22] L. Canet, H. Chaté, B. Delamotte, and C. Gombaud (unpublished).

[23] H. Arisue, T. Fujiwara, and K. Tabata, Nucl. Phys. B, Proc. Suppl. **129**, 774 (2004).

[24] M. D'Attanasio and T. R. Morris, Phys. Lett. B **409**, 363 (1997).

[25] J. Zinn-Justin, *Quantum Field Theory and Critical Phenomena* (Clarendon, Oxford, 2002).

[26] M. Moshe and J. Zinn-Justin, Phys. Rep. **385**, 69 (2003).

[27] A. A. Pogorelov and I. M. Suslov, JETP **105**, 360 (2007).

[28] G. v. Gersdorff and C. Wetterich, Phys. Rev. B **64**, 054513 (2001).

[29] A. A. Pogorelov and I. M. Suslov, J. Exp. Theor. Phys. **106**, 1118 (2008).

[30] P. Grassberger, P. Sutter, and L. Schäfer, J. Phys. A **30**, 7039 (1997).

[31] M. Hasenbusch, Phys. Rev. B **82**, 174433 (2010).

[32] M. Campostrini, M. Hasenbusch, A. Pelissetto, and E. Vicari, Phys. Rev. B **74**, 144506 (2006).

[33] M. Campostrini, M. Hasenbusch, A. Pelissetto, P. Rossi, and E. Vicari, Phys. Rev. B **65**, 144520 (2002).

[34] R. Guida and J. Zinn-Justin, J. Phys. A **31**, 8103 (1998).

[35] M. Hasenbusch, J. Phys. A **34**, 8221 (2001).

[36] S. A. Antonenko and A. I. Sokolov, Phys. Rev. E **51**, 1894 (1995).

[37] A. Pelissetto and E. Vicari, J. Phys. A **40**, F539 (2007).

[38] J.-P. Blaizot, R. Mendéz Galain, and N. Wschebor, Europhys. Lett. **72**, 705 (2005).

[39] G. Baym, J.-P. Blaizot, M. Holzmann, F. Laloe, and D. Vautherin, Phys. Rev. Lett. **83**, 1703 (1999).

[40] G. Baym, J.-P. Blaizot, and J. Zinn-Justin, Europhys. Lett. **49**, 150 (2000).

[41] S. Ledowski, N. Hasselmann, P. Kopietz, Phys. Rev. A **69**, 061601(R) (2004).

[42] B. M. Kastening, Phys. Rev. A **69**, 043613 (2004).

[43] X. Sun, Phys. Rev. E **67**, 066702 (2003).

[44] P. Arnold and G. Moore, Phys. Rev. Lett. **87**, 120401 (2001).

[45] V. A. Kashurnikov, N. V. Prokof'ev, and B. V. Svistunov, Phys. Rev. Lett. **87**, 120402 (2001).

[46] V. Martin-Mayor, A. Pelissetto, and E. Vicari, Phys. Rev. E **66**, 026112 (2002).

[47] M. E. Fisher and J. S. Langer, Phys. Rev. Lett. **20**, 665 (1968).

[48] A. J. Bray, Phys. Rev. B **76**, 1248 (1976).

[49] P. Damay, F. Leclercq, R. Magli, F. Formisano, and P. Lindner, Phys. Rev. B **58**, 12038 (1998).

[50] R. A. Ferrell and D. J. Scalapino, Phys. Rev. Lett. **34**, 200 (1975).

[51] M. Campostrini, A. Pelissetto, P. Rossi, and E. Vicari, Phys. Rev. E **65**, 066127 (2002).

[52] N. Dupuis, Phys. Rev. A **80**, 043627 (2009).

[53] M. Caselle, M. Hasenbusch, P. Provero, and K. Zarembo, Nucl. Phys. B **623**, 474 (2002).

[54] L. Canet, H. Chaté, B. Delamotte, and N. Wschebor, Phys. Rev. Lett. **104**, 150601 (2010).

[55] L. Canet, H. Chaté, B. Delamotte, and N. Wschebor, Phys. Rev. E **84**, 061128 (2011).

[56] A. Pelissetto and E. Vicari, Phys. Rep. **368**, 549 (2002).